Deutsches Zentrum
für Luft- und Raumfahrt
German Aerospace Center

CONSTRUCTOR
UNIVERSITY

Constructor University Bremen
School of Science

Optimizing Energy Dispatch Leveraging Uncertainty Information in Short-Term Wind Power Forecasts

BSc Thesis in Physics

as part of the module
CA-PHY-800 Bachelor Thesis Physics

by

Clara Elisabeth Buller

Supervised by Dr. Lüder von Bremen

Second reader: Prof. Dr. Stefan Kettemann

Abstract

To adapt to the increasing share of renewable producers in power systems, the energy dispatch has to be redesigned to consider the intermittent nature of renewable energy sources and its predictability. A stochastic dispatch model was tested for optimizing the energy dispatch in the day-ahead market, which implements expected balancing costs using ensemble forecasts in a two-stage stochastic market clearing. It was compared to a conventional dispatch model, which bases its day-ahead market clearing on a deterministic forecast. The impact of the level and spatial distribution of generator flexibility and of link capacities was analyzed for both models.

The results of the thesis show that the stochastic dispatch model improves the overall market performance. It decreases total system costs from 2.72€/MWh in the conventional dispatch model to 2.38€/MWh equalling yearly total savings of 47.5 Mio€. It decreases curtailment slightly by 4000 MWh from 184.4×10^5 to 184.0×10^5 MWh. It significantly improves shedding by reducing the total amount of shedded load by 317000 MWh from 318034 MWh in the conventional model to 1448 MWh with a total load of ca. 140×10^6 MWh.

Increased generator flexibility level reduces the total amount of shedded load significantly for both models, where it is ideal to locate the generator with the highest generator flexibility at the bus with the highest load. Increasing link capacity of links connected from a bus with a high share of wind power to a bus with a high load, decreases overall curtailment. This results in increased system costs for the conventional model due to increased shedding as the deterministic forecast is less accurate in predicting sudden downward ramps in wind power, which trigger shedding. In the stochastic model total system costs are decreased as it utilizes successfully more wind energy with marginal costs of 0€/MWh using the ensemble forecast.

Contents

Nomenclature

Sets

$i \in \mathcal{I}$ Set of sectors

$I \in \mathcal{L}$ Set of links

$n \in \mathcal{N}$ Set of buses

$s \in \mathcal{S}$ Set of carrier types

Parameters

$\overline{F}_{\mathrm{I}}$ Nominal link capacity

$\overline{G}_{\mathrm{n,s}}$ Nominal generator capacity

$\tilde{G}_{\mathrm{n,s,t}}$ Availability (forecasted) of generator

$\tilde{G}^{\mathrm{obs}}_{\mathrm{n,s,t}}$ Availability (observed) of generator

$C^{+}_{\mathrm{n,s}}$ Cost of balancing dispatch deficit

$C^{-}_{\mathrm{n,s}}$ Cost of balancing dispatch surplus

$C^{\mathrm{shed}}_{\mathrm{i}}$ Cost of load shedding

$K_{\mathrm{n,I}}$ Incidence Matrix of network topology

$L_{\mathrm{n,i,t}}$ Load at bus n in sector i at time t

$O_{\mathrm{n,s}}$ Marginal price

W_{t} Snapshot weighting

Decision Variables

$f_{\mathrm{I,t}}$ Link capacity

$g^{*}_{\mathrm{n,s,t}}$ Optimal day-ahead dispatch

$g^{+}_{\mathrm{n,s,t},\omega}$ Balancing dispatch deficit

$g^{+}_{\mathrm{n,s,t},\omega}$ Balancing dispatch surplus

$g^{\mathrm{curt}}_{\mathrm{n,s,t},\omega}$ Curtailed generation

$g_{\mathrm{n,s,t}}$ Day-ahead dispatch

$l^{\mathrm{shed}}_{\mathrm{n,s,t},\omega}$ Shedded load

Constants

$C^{\mathrm{B}}_{\mathrm{conv.}}$ Costs conv. balancing market

$C^{\mathrm{B}}_{\mathrm{stoch.}}$ Costs stoch. balancing market

$C^{\mathrm{conv.}}$ Total costs conventional model

$C^{\mathrm{D}}_{\mathrm{conv.}}$ Costs conv. day-ahead market

$C^{\mathrm{D}}_{\mathrm{stoch.}}$ Costs stoch. day-ahead market

$C^{\mathrm{stoch.}}$ Total costs stochastic model

1 Introduction

One of the key issue of today's world is to combat climate change in an efficient and timely manner before the threshold of a global warming of 1.5°C is reached, which will result in irreversible consequences [1].

The global energy sector as the largest emitter of CO2 is one of the main drivers of the climate crisis [2]. According to the Net Zero Emissions by 2050 (NZE) scenario of the International Energy Agency (IEA) the installed share of renewable energy has to rise from 28% in 2021 to over 60% in 2030 and eventually reach nearly 90% in 2050 [3]. New policies, technologies and operational methods have to be developed to sustainably accommodate the globally increasing electricity demand. Hence, the energy transition - away from conventional fossil fuel power plants towards renewable energy sources - has to be of utmost priority and yet presents a major challenge.

A rapidly growing share of renewable energy sources in the electricity market leads to elevated penetration levels of renewable producers with a very volatile energy input in the electricity market. Here, a significant contributor are wind power plants. As an already mature technology it has demonstrated high competitiveness with conventional power plants [4].

Due to the weather dependent nature of renewable energy sources the uncertainty of the system increases. Their energy production is variable on all time scales from milliseconds to months and years [5]. For stochastic fluctuations on time scales below 15 minutes ancillary balancing methods (e.g. automatic- and manual frequency restoration reserves (aFRR, mFFR) [6]) and new forms of momentary reserves (e.g. grid-forming inverters [7]) have to be implemented to maintain a stable power grid.
However, the focus of this thesis is on variations on larger time scales of hours, days to months. Here, a promising approach is to reform the electricity market design and adapt new dispatch methods. It is essential for wind power and other volatile renewable energy sources to replace more and more conventional energy sources in a cost-efficient manner while maintaining the overall stability of the energy system [8].

On the supply side, solutions to account for the increased uncertainty in generation include an international expansion of the transmission grid [9] [10]. This removes system constraints and allows for spatial balancing of fluctuations by stochastic producers. Further, temporal balancing can be achieved by integrating highly efficient storage technologies [9]. Another approach is to pool different energy sources into virtual power plants and increase the overall resilience based on their complementary nature [11].

On the demand side, e.g., sector-coupling meaning the connecting of energy consuming sectors (like heating, transport, industry) with the energy producing sector has been proposed to increase flexibility. Especially significant flexibility contributions were found from technologies like battery electric vehicles (BEV), power-to-gas units (P2G) and long-term thermal energy storage (LTES) [12].

This thesis will focus on implementing and analyzing a market scheme proposed by J. M. Morales [13], which explicitly incorporates the uncertainty in short-term forecasting of renewable energy sources using probabilistic ensemble forecasting via a two-stage stochastic programming market clearing. It is based on a simplified energy market, which consists of a day-ahead market, where producers determine the electricity dispatch one day prior to delivery, and a balancing procedure to restore balance due to deviations in predicted and actual generations by wind power plants.

Conventionally, the day-ahead market and the balancing measures are considered independently in a process called separate bidding. The day-ahead market is cleared using a least-merit order based on a deterministic forecast. Hence, as stochastic producers like a wind park enters the market with very low marginal costs of usually zero, they are being dispatched first. But these forecasts are inherently inaccurate when describing a stochastic system and occurring forecasting errors have to be compensated with balancing energy for an increased price [13].

Morales' two-stage stochastic market clearing takes the expected costs occurring in balancing into account using probabilistic weather forecasts in a process called optimal bidding. This allows to endogenously determine the amount of reserve capacities needed for balancing [13]. In the first stage - the here-and-now decisions - the day-ahead dispatch schedule is determined, while in the second stage - the wait-and-see decisions - the real time operation of the power system is considered. Hence, it displays the interaction between the day-ahead market and the balancing process and determines the optimal energy dispatch by anticipating the balancing operations using network and grid constraints and the expected balancing costs to maximize market efficiency [14].

The objective of this thesis is to investigate I) how the proposed stochastic market-clearing procedure compares to the conventional method of market-clearing using deterministic forecast in terms of efficiency and cost-effectiveness. Furthermore, it II) examines how factors such as provided generator flexibility and link capacity contribute to the performance of the model. The findings of the thesis can improve our understanding of how to design a more efficient and sustainable energy market that incorporates the uncertainty in short-term wind power forecasts, which is essential for achieving the transition to a low-carbon future.

2 Theory

2.1 Probabilistic Forecasting

The atmosphere is a chaotic system. That means its future state cannot be described with unlimited accuracy as its evolution is highly sensitive to its initial conditions [15][16]. Hence, all forecasts are inherently uncertain. There are two main sources of uncertainty: 1) the assumptions underlying the deterministic physical laws describing the atmosphere and 2) the uncertainty in the configuration of the initial state. In order to display the uncertainty in forecasts, probabilistic forecasts have been developed, which consider this uncertainty by applying the physical laws to a probability distribution of the initial state [15]. The distribution represents a full range of possible initial states, and hence its result reflects a range of possible outcomes. This makes it a more complete representation than a single deterministic forecast.

In Stochastic Dynamic Forecasting this probability distribution moves through the phase space - a geometrical representation of all hypothetically possible states - following the laws of fluid dynamics. As time progresses, the initial distribution becomes more distorted and dispersed for longer projections. This is equivalent to higher uncertainty in forecasts further into the future. However, the equations describing this evolution are too large to be solved directly due to the dimensionality of phase space when considering realistic problems with an actual forecasting interest [15]. A solution is offered by ensemble forecasts. Here, only a finite set of representative members are picked, where each member represents one initial state configuration. Now, the movement of the probability distribution is approximated via the collective trajectories of the ensemble members through phase space [15]. There are different ways of efficiently selecting initial members. The ensemble forecasts used in this thesis are from the European Centre for Medium-Range Weather Forecasts (ECMWF) [17]. They are generated using singular vectors. They identify the direction of uncertainty in the initial state, that results in the largest uncertainty of the model state at a time t in the future [18]. Ensemble members are then defined using linear combinations of the identified patterns, with their magnitude corresponding to the level of analysis uncertainty [15].

2.2 Optimal Power Flow Model

This thesis is based on the Optimal Power Flow (OPF) Model under DC-Approximation (DC-OPF), an important approach for electricity system modelling. It is a simplification of the AC-OPF, which is a non-linear, non-convex optimization problem [19]. Its goal is to minimize an objective function - the cost function - while considering physical, operational and technical constraints of the network. This includes among others Ohm's - and Kirchhoff's laws, operational limits of generators, capacity limits of links and voltage levels [20].
Mathematically, it can be expressed as follows [19]:

$$\begin{aligned} & \min_{y} f(x,y) \\ s.t. \quad & c_i^E(x,y) = 0 \quad i = 1,...,n \\ & c_j^I(x,y) \geq 0 \quad j = 1,...,m \end{aligned} \tag{2-1}$$

Here, x denotes the grid parameter - and y the optimization variable vector. They are the arguments for $f(x, y)$ - the objective function, which has to be minimized, while being subject to n equality constraints $c_i^E \in C^E$ and m inequality constraints $c_j^I \in C^I$.
The AC-OPF power flow equation considers both active and reactive power flow [20][21]. Consider a set of buses $\mathcal{N}$, which are connected by transmission lines with the index $I \in \mathcal{L}$. Then the complex power flow S_{ij} from bus i to bus j can be decomposed into its active (p_{ij}) and reactive components (q_{ij}). Following the derivation of [22] they can be expressed in case of the simple power flow model as:

$$p_{ij} = \frac{1}{r_{ij}^2 + x_{ij}^2}[r_{ij}(v_i^2 - v_i v_j \cos(\delta_{ij})) + x_{ij}(v_i v_j \sin(\delta_{ij}))] \tag{2-2}$$

$$q_{ij} = \frac{1}{x_{ij}^2 + x_{ij}^2}[r_{ij}(v_i^2 - v_i v_j \cos(\delta_{ij})) + x_{ij}(v_i v_j \sin(\delta_{ij}))] \tag{2-3}$$

where r_{ij} is the resistance of each transmission line, x_{ij} the line reactance, and v_i and δ_j the voltage magnitude and voltage angle at bus i, respectively. While the full AC power flow equations is more accurate, it is also more likely to diverge and can be up to 60 times slower. Hence, the DC-OPF makes the following assumption to consider a linearized power flow only [21][23]:

- The resistance of each line r_{ij} is negligible relative to line reactance x_{ij}, and hence can be assumed to be $r_{ij} \approx 0$.
- The bus voltage magnitudes are approximated by one per unit such that $v_i \approx 1$.
- The voltage angle difference of each branch $\delta_{ij} << 1$, i.e. $\cos(\delta_{ij}) \approx 1$ and $\sin(\delta_{ij}) \approx \delta_{ij}$.

Applying these assumptions results in this simplified final form:

$$p_{ij} \approx \frac{\delta_{ij}}{x_{ij}} = f_{\mathrm{I}} \tag{2-4}$$

$$q_{ij} \approx 0 \tag{2-5}$$

The physicality of the flows described in equation 2-4 is ensured by implementing the Kirchhoff's current law also called node-balance equation, which states that the power reaching each bus must equal the power withdrawn from the bus at all time steps t. Using the incidence matrix $\mathbf{K}$, which is defined as follows:

$$\mathbf{K}_{\mathrm{i,j}} = \begin{cases} 1, & \text{if transmission link I begins at node } i \\ -1, & \text{if transmission link I ends at node } i \\ 0, & \text{otherwise} \end{cases} \tag{2-6}$$

and a reactance value of x_{ij}, the flows can be expressed per time step as:

$$f_{\mathrm{I}} = \sum_{i,j} \frac{k_{ij}\delta_{ij}}{x_{,j}} \tag{2-7}$$

Implementing Kirchhoff's current law results in the following expression for p_{ij}, the net active power being the difference between consumption and generation at bus i [24].

$$p_{ij} = \sum_{I} k_{ij} f_{\mathrm{I}} \tag{2-8}$$

Together with the remaining constraints, it leaves a linear objective function, which can be solved very efficiently as a linear programming problem [22].

2.3 Energy Dispatch Models

An energy dispatch model is used to manage the operation schedule of all generators within a power system network. Considering factors like short-term weather forecasts and cost of electricity, it optimizes the allocation of available energy sources to meet the demand as efficiently as possible meaning while minimizing the costs of the electricity market.

In this thesis costs can occur at two stages in the electricity market. First, in the day-ahead market, which is cleared one day prior to delivery $(d-1)$ and determines a typically hourly dispatch schedule. Second, in the balancing process, where any imbalances between day-ahead schedule and actual energy production are settled in real-time [13].

This thesis compares two energy dispatch models, the conventional dispatch model and the stochastic dispatch model, which are both formulated as a DC-OPF.

2.3.1 Conventional Dispatch Model

In the conventional dispatch model the day-ahead and balancing are settled separately in a sequential market bidding process. Consider a network consisting of a set of buses $\mathcal{N}$, which are connected by links denoted as $I \in \mathcal{L}$. The time-dependent load per bus n in sector i ($i \in \mathcal{I} = \{$Industry; Commerce, Trade, Services (CTS); Domestic$\}$) at time t is denoted as $L_{\mathrm{n,i,t}}$. Without loss of generality, it is assumed that the demand at each bus is known with certainty. The load can be covered by the electricity generated by generators based on the carrier $s \in \mathcal{S}$ with $\mathcal{S} = \{$Onshore wind park (WP), Offshore WP, OCGT$\}$. Here, $g_{\mathrm{n,s,t}}$ denotes the electricity covered by generator with carrier type s at bus n at time t in the day-ahead schedule. Each generator is assigned a marginal cost $O_{\mathrm{n,s}}$, which is assumed to be time-independent. Costs related to investments are not considered as it is assumed that all necessary investments have been carried out already and no expansion planning is being done. Generation is limited by the nominal power $\overline{G}_{\mathrm{n,s}}$ as well as the forecasted availability of the power source $\tilde{G}_{\mathrm{n,s,t}}$. For a stochastic producer this depends on meteorological conditions (here: wind speed), whereas for conventional producer it is a constant.
Now, the electricity needs to be distributed from the buses, where it is generated, to the buses, where it is consumed. This is done via transmission links, which each are assigned a nominal capacity $\overline{F}_I$. Here, no costs related to investment or transmission losses are assumed.

Based on this, the problem of minimising day-ahead costs $C^{\mathrm{D}}_{\mathrm{conv.}}$ can be mathematically formulated as follows:

$$C^{\mathrm{D}}_{\mathrm{conv.}} = \min_{g_{\mathrm{n,s,t}}} \left[\sum_{n} \sum_{s} \sum_{t} (W_{\mathrm{t}} O_{\mathrm{n,s}} g_{\mathrm{n,s,t}}) \right] \tag{2-9}$$

Equation 2-9 is used throughout the thesis as the cost function of the conventional dispatch model. The electricity dispatch $g_{\mathrm{n,s,t}}$ is the decision variable. W_{t} are optional snapshot weightings, where each snapshot represents one time step. This can be used to represent the probability of different load/weather conditions [25]. Additionally, the incidence matrix $K_{\mathrm{n,I}}$ describing the topology of the network, the load $L_{\mathrm{n,i,t}}$ and the forecasted availability $\tilde{G}_{\mathrm{n,s,t}}$ are entered as exogenous data.

The cost function is subject to several constraints:

1. Nodal balancing: At each node n during every time step t, the generated electricity has to be equal to the load.

$$\sum_{s} g_{\mathrm{n,s,t}} - \sum_{I} K_{\mathrm{n,I}} f_{\mathrm{I,t}} - L_{\mathrm{n,i,t}} = 0 \quad , \forall n, s, t, I \tag{2-10}$$

2. Upper bound: Generation cannot exceed available nominal power.

$$g_{\mathrm{n,s,t}} - \tilde{G}_{\mathrm{n,s,t}} \cdot \overline{G}_{\mathrm{n,s}} \leq 0 \quad , \forall n, s, t \tag{2-11}$$

3. Declaration of non-negative variables.

$$0 \leq g_{\mathrm{n,s,t}} \quad , \forall n, s, t \tag{2-12}$$

$$0 \leq |f_{\mathrm{I,t}}| \leq \overline{F}_{\mathrm{I}} \quad , \forall n, s, t \tag{2-13}$$

The generators are dispatched in a least-cost merit-order principle following the concept of a network-constrained auction. As stochastic producers have very low marginal costs of mostly 0, they will usually be dispatched first.
After the optimal day-ahead schedule $g^{*}_{\mathrm{n,s,t}}$ has been found as the solution of the optimization problem, it is used as an input to balance any deviations between the schedule $g^{*}_{\mathrm{n,s,t}}$ and the realization of the energy production $\tilde{G}^{\mathrm{obs}}_{\mathrm{n,s,t}}$ (in comparison to the forecasted availability $\tilde{G}_{\mathrm{n,s,t}}$).

In case of a deviation the following measures can be taken:

- Increase or decrease electricity generation of flexible producers by $g^{+}_{\mathrm{n,s,t}}$ or $g^{-}_{\mathrm{n,s,t}}$ bounded by the available flexibility $\eta^{\pm}_{\mathrm{n,s}}$ in case of an deficit or excess of (wind) production, respectively. Each process is assigned a corresponding cost ($C^{+}_{\mathrm{n,s}}$, $C^{-}_{\mathrm{n,s}}$). In case the wind power is lower than forecasted and OCGT generators have to increase generation, they get paid $C^{+}_{\mathrm{n,s}}$ per MWh, which is higher than the day-ahead price by a defined cost premium. In case the wind power is higher than forecast, the OCGT generators have to decrease the previously scheduled generation. In this scenario, the OCGT provider pays back the money they received in the day-ahead market reduced by the defined cost premium and $C^{-}_{\mathrm{n,s}}$ enters the cost function with a negative sign.

- Shedding part $l^{\text{shed}}_{\text{n,t,i}}$ of the load at a cost of $C^{\text{shed}}_{\text{i}}$ depending on the sector i. This is usually the most expensive measure.

Further, a part $g^{\text{curt}}_{\text{n,s,t}}$ of the wind production can be curtailed but as this is not connected to costs, it is not a decision variable of the optimization problem. Hence, the costs $C^{\text{B}}_{\text{conv.}}$ associated with the balancing process can be summarized as follows.

$$\min_{g^+,g^-,l^{\text{shed}}} \sum_{\text{n,s,t}} (g^+_{\text{n,s,t}} C^+_{\text{n,s}} - g^-_{\text{n,s,t}} C^-_{\text{n,s}}) + \sum_{n,t,i} (l^{\text{shed}}_{\text{n,t,i}} C^{\text{shed}}_{\text{i}}) \tag{2-14}$$

s.t.

$$\sum_s (g^+_{\text{n,s,t}} - g^-_{\text{n,s,t}}) + \sum_i l^{\text{shed}}_{\text{n,t,i}} - (L_{\text{n,i,t}} - g^*_{\text{n,s,t}}) = 0, \quad \forall n, s, t, il \tag{2-15}$$

$$(g^*_{\text{n,s,t}} + g^+_{\text{n,s,t}} - g^-_{\text{n,s,t}}) - (\tilde{G}_{\text{n,s,t}} \overline{G}_{n,s}) \leq 0, \quad \forall n, s, t \tag{2-16}$$

$$g^*_{\text{n,s,t}} - g^-_{\text{n,s,t}} \leq 0, \quad \forall n, s, t \tag{2-17}$$

$$g^*_{\text{n,s,t}} + g^+_{\text{n,s,t}} \leq \tilde{G}^{\text{obs}}_{\text{n,s,t}} \overline{G}_{\text{n,s}}, \quad \forall n, s, t \tag{2-18}$$

$$g^-_{\text{n,s,t}} \leq \overline{G}_{\text{n,s}} \eta^+_{\text{n,s}}, \quad \forall n, s, t \tag{2-19}$$

$$g^+_{\text{n,s,t}} \leq \overline{G}_{\text{n,s}} \eta^-_{\text{n,s}}, \quad \forall n, s, t \tag{2-20}$$

Equation 2-15 ensures that the redispatching of generators and loads are done such that it exactly compensates the deviation between day-ahead schedule and realization. Equation 2-17 defines that in order to provide negative reserve the generator needs to run at least on that level but neglects a minimum load requirement. Similarly, equation 2-18 defines that a generator providing positive reserves does not surpass its available power. Equation 2-19 and 2-20 ensure that the provided balancing does not surpass the flexibility of the generator. Additionally, the non-negative condition (Eq. 2-12, Eq. 2-13) still applies.

Note, that the optimal day-ahead schedule $g^*_{\text{n,s,t}}$ is used as an input parameter for $C^{\text{B}}_{\text{conv.}}$ and thus, does not capture any dependency. The overall cost for the conventional system is given by:

$$C^{\text{conv.}} = C^{\text{D}}_{\text{conv.}} + C^{\text{B}}_{\text{conv.}} \tag{2-21}$$

This derivation followed similar formulations in [13], [24] and [26].

2.3.2 Stochastic Dispatch Model

The stochastic dispatch model is based on probabilistic forecasting to capture the interaction between day-ahead market and balancing. Following the formulation in [13], a set of Ω scenarios each based on a member of an ensemble forecast is assumed. Every member $\omega \in \Omega$ is associated with forecasted available wind power $\tilde{G}_{\text{n,s,t},\omega}$ with $s \in \{\text{onshore, offshore}\}$ and a probability of occurrence π_ω. Hence, $\pi_\omega \geq 0, \quad \forall \omega \in \Omega$ and $\sum_\omega \pi_\omega = 1$. Now, the expected balancing costs $\mathbb{E}[C^{\text{B}}]$ is immediately considered in the cost function $C^{\text{D}}_{\text{stoch.}}$:

$$\min_{g,g^+,g^-,l^{\text{shed}}} \sum_{n,s,t} (W_{\text{t}} O_{\text{n,s}} g_{\text{n,s,t}}) + \mathbb{E}\left[\sum_{n,s,t,\omega} (g^+_{\text{n,s,t},\omega} C^+_{\text{n,s}} - g^-_{\text{n,s,t},\omega} C^-_{\text{n,s}}) + \sum_{n,t,i,\omega} (l^{\text{shed}}_{\text{n,i,t},\omega} C^{\text{shed}}_{\text{i}}) \right] \tag{2-22}$$

s.t.

$$\sum_{n,s,t,\omega} (g_{\mathrm{n,s,t}} + g^{+}_{\mathrm{n,s,t,\omega}} - g^{-}_{\mathrm{n,s,t,\omega}}) + \sum_{n,i,t,\omega} l^{\mathrm{shed}}_{\mathrm{n,t,i,\omega}} - (L_{\mathrm{n,i,t}} - g^{*}_{\mathrm{n,s,t}}) - \sum_{I} K_{\mathrm{n,I}} f_{\mathrm{I}} = 0, \quad \forall n, s, t, \omega \in \Omega \tag{2-23}$$

$$0 \leq g_{\mathrm{n,s,t}}, \quad \forall n, s, t \tag{2-24}$$

$$0 \leq |f_{\mathrm{I,t}}| \leq \overline{F}_{\mathrm{I,t}}, \quad \forall I, t \tag{2-25}$$

$$(g^{*}_{\mathrm{n,s,t}} + g^{+}_{\mathrm{n,s,t,\omega}} - g^{-}_{\mathrm{n,s,t,\omega}}) - (\tilde{G}_{\mathrm{n,s,t}} \overline{G}_{\mathrm{n,s}}) \leq 0, \quad \forall n, s, t, \omega \in \Omega \tag{2-26}$$

$$g^{*}_{\mathrm{n,s,t}} - g^{-}_{\mathrm{n,s,t,\omega}} \leq 0, \quad \forall n, s, t, \omega \in \Omega \tag{2-27}$$

$$g^{*}_{\mathrm{n,s,t}} + g^{+}_{\mathrm{n,s,t,\omega}} \geq \tilde{G}_{\mathrm{n,s,t}} \overline{G}_{\mathrm{n,s,t}}, \quad \forall n, s, t, \omega \in \Omega \tag{2-28}$$

$$g^{-}_{\mathrm{n,s,t,\omega}} \leq \overline{G}_{\mathrm{n,s}} \eta^{+}_{\mathrm{n,s}}, \quad \forall n, s, t \tag{2-29}$$

$$g^{+}_{\mathrm{n,s,t,\omega}} \leq \overline{G}_{\mathrm{n,s}} \eta^{-}_{\mathrm{n,s}}, \quad \forall n, s, t \tag{2-30}$$

Note, that equation 2-23 ensures that the nodal balance equation is fulfilled, conditions 2-24 to 2-25 ensure that the day-ahead schedule is feasible, while 2-23 to 2-28 model the expected balancing action and ensure its feasibility. Further, 2-29 and 2-30 ensures that balancing is bounded by the available flexibility. Hence, this maximizes overall market efficiency. After determining the optimal day-ahead schedule $g^{*}_{\mathrm{n,s,t}}$, again balancing is calculated following the description in 2-14 to 2-20. As in the conventional model the costs of both markets combined make up total system costs for the stochastic dispatch model:

$$C^{\mathrm{stoch.}} = C^{\mathrm{D}}_{\mathrm{stoch.}} + C^{\mathrm{B}}_{\mathrm{stoch.}} \tag{2-31}$$

3 Methodology

3.1 Network Design

A visualization of the implemented power system network can be found in Fig. 1. It is a fit to purpose power network of northern Germany with main buses in Büttel, Hamburg, Wilhelmshaven and Ems, an area with typically very high penetration of wind energy in Germany [27]. The network is connected to the Ruhrgebiet, a highly industrialized region with high demand and high conventional power production. Only two of the German offshore wind park clusters (Hohe See and Sandbank) have been selected and are considered in the network. Additionally, the wind park Nordergründe was included in the network. The offshore wind parks are connected to the closest bus (Hohe See and Ems, Sandbank and Büttel, Nordergründe and Wilhelmshaven) and for simplicity, their grid capacity is set to the capacity of the connected offshore wind farms. Their capacity was set in relation to the load at the connected buses and not to real-life values.

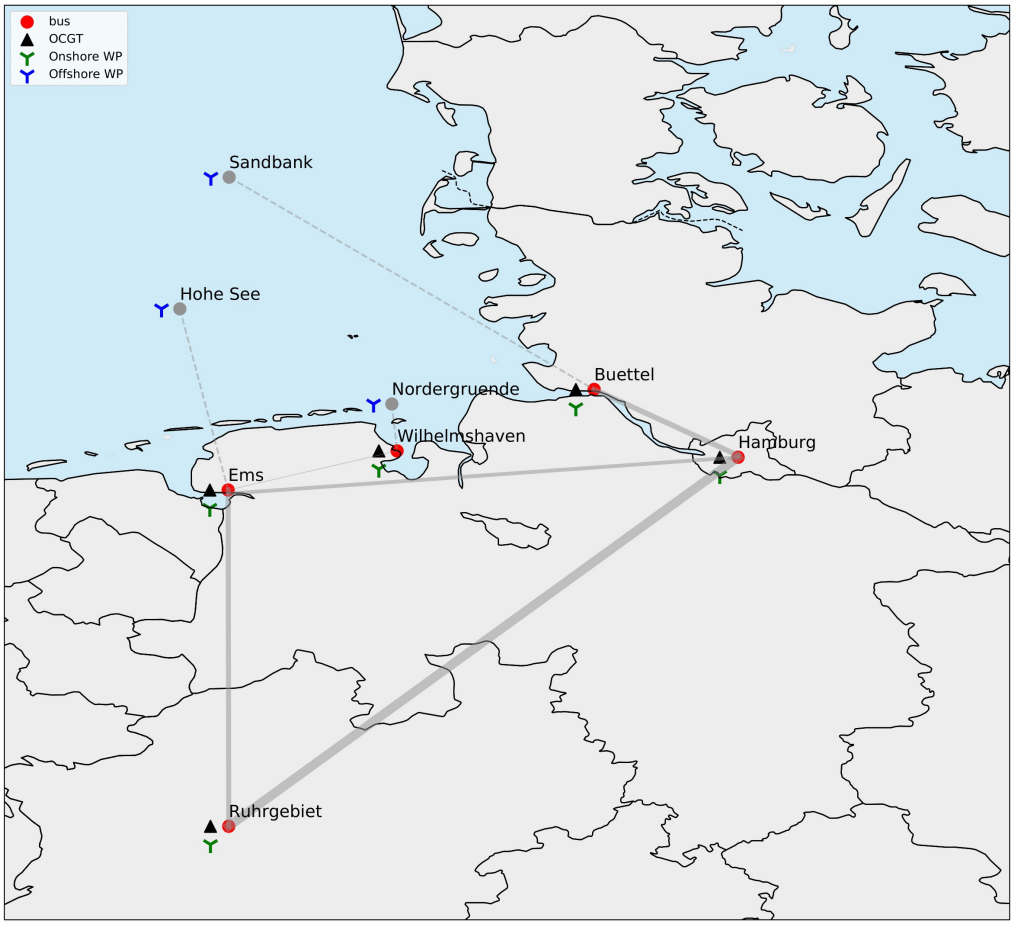

Figure 1: Visualization of power system network used in thesis. Thickness of links corresponds their nominal capacity. Connection between offshore wind parks and corresponding buses are marked by thin, grey dashed line.

The amount of needed energy also called load was determined by using electricity demand data of the Open Energy Tracker [28]. The load at each bus can be split into three sectors: Domestic, CTS (Commerce, Trade, Services) and Industry. The values for Hamburg are taken directly from Open Energy Tracker [28], which provides load values per federal state in Germany divided by sector. For the remaining values, the total amount of load was determined in relation to Hamburg (Table 1) and the ratio between the sectors was taken from the Open Energy Tracker as the ratio of the sectors in the corresponding federal state of the bus. In case of an underproduction of energy one measure is to shed part $l^{\text{shed}}_{\text{n,t,i}}$ at the sector i specific cost $C^{\text{shed}}_{\text{i}}$. The cost is staggered with shedding the household load being the most expensive measure at 250€/MWh, followed by CTS at 200€/MWh and eventually, the industrial load at 150€/MWh. The values were chosen to display the effect that shedding is relatively the most expensive balancing measure as well as the differences in shedding cost per sector and not based on loss of load cost in reality.

	Sector	Hamburg	Büttel	Ems	Wilhelmshaven	Ruhrgebiet
Total load rel. to HH	-	1	0.1	0.15	0.3	10
Avg. Load [MWh]	Domestic	436.2	58.7	51.3	104.0	3447.8
	CTS	455.9	46.0	57.7	117.0	3009.1
	Industry	534.0	38.7	101.8	206.3	7269.6
Peak Load [MWh]	Domestic	801.4	107.9	94.2	191.0	6334.8
	CTS	948.6	120.1	57.7	243.4	6260.7
	Industry	621.7	45.1	118.5	240.1	8642.7

Table 1: Definition, average and peak of load

Furthermore, using the demandlib Python library load profiles for each bus and sector were implemented in form of a time series. This allows to consider effects such as working days and hours, holidays and seasonality. An example of the load profile of an average day during winter (a) as well as the seasonal cycle (b) can be found in Fig. 2.

In general, three carriers for generators are considered: On- and offshore wind parks (WP) as stochastic producers and open-cycle gas turbines (OCGT) as conventional producers, each assigned a nominal capacity $\overline{G}_{\text{S}}$ (Table 2). The marginal costs are 0€/MWh for wind parks and 4.50€/MWh for OCGTs at the day-ahead market. Each OCGT is taken as a flexible generator meaning it is capable in case of imbalances to either in- or decrease its production by 20% and 40% of its $\overline{G}_{\text{n,s}}$, respectively during balancing. As this requires the provision of reserves and flexibility for short-term trading, it increases overall system costs. This is

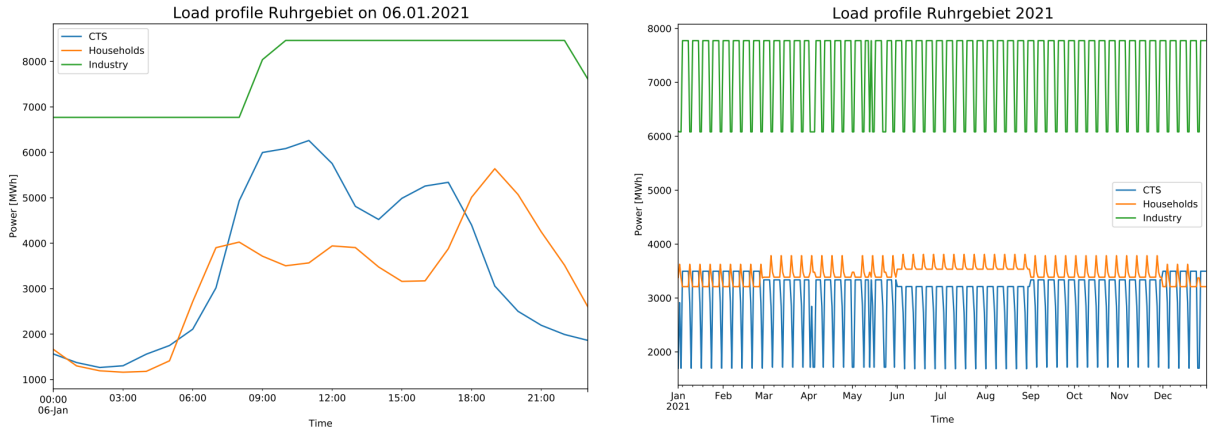

(a) Daily load profile

(b) Yearly load profile

Figure 2: Examples of implemented load profile for Ruhrgebiet

implemented through a cost premium for balancing, which is 14% for an upwards correction meaning it sells at 1.14-times the day-ahead price. In case of a downwards correction a price premium of 3% is implemented meaning only 97% of the price received at the day-ahead market is paid back by the OCGT generator providers. Furthermore, the values of $\overline{G}_{\mathrm{n,s}}$ were chosen to roughly display real-world capacities of the buses as well as to showcase behavior of future systems. It was made sure that the capacity of the conventional generators is able to cover the entire demand by setting it to 105% of the peak load of the load time series. This was done to avoid having an infeasible solution for the conventional dispatch model. The offshore wind nominal capacity was set in relation to the average of the total load of Hamburg (e.g. offshore wind park Ems: 0.15-times Hamburg's average total load). The remaining onshore nominal capacity values were defined in relation to the load of the bus and considering an onshore-capacity factor being the ratio of actually generated electricity and theoretical maximum of 0.25 (e.g. onshore wind park Wilhelmshaven: 25% of 1.5-times Wilhelmhaven's average load).

	Carrier	Büttel	Hamburg	Ems	Wilhemshaven	Ruhrgebiet
Nom. Capacity $\overline{G}_{\mathrm{n,s}}$ [MW]	onshore WP	2996.57	119.87	2689.72	2696.91	5993.15
	offshore WP	4494.86	-	7491.42	449.48	-
	OCGT	216.41	2122.62	306.19	620.65	19280.30

Table 2: Nominal capacity of generators $\overline{G}_{\mathrm{n,s}}$

Between each bus links with the nominal capacity $\overline{F}_{\mathrm{I}}$ (Table 3) are used to transport the energy. It was chosen in relation to the connected on- and offshore wind power s.t. among other bottleneck behaviour can appear to investigate its impact on the model performance.

For this $\overline{F}_1$ is set to 50% of the wind power capacity connected to Büttel, $\overline{F}_2$ is set to the sum of the nominal capacity of Büttel-HH and HH-Ems. $\overline{F}_3$ covers 20% of wind power capacity in Ems and Wilhelmshaven, while $\overline{F}_4$ is equal to 25% of the connected wind power capacity in Wilhelmshaven and Ems. $\overline{F}_5$ is set to the nominal capacity of the offshore wind park Nordergründe in Büttel.

	Büttel-HH (1)	HH-Ruhr (2)	HH-Ems (3)	Ems-Ruhr. (4)	Ems-Whv (5)
Nom. Capacity $\overline{F}_\mathrm{I}$ [MW]	3567.35	6105.94	2538.58	3346.82	428.08

Table 3: Nominal capacity of links $\overline{F}_\mathrm{I}$

3.2 Technical Implementation

Using above mentioned parameters a network model was built using the open-source software *Python for Power System Analysis* (PyPSA). It carries out the optimal load flow linearization described in 2.2 to solve the optimization problem and find the day-ahead schedule with minimal system costs for both models using the cost function 2-9 and 2-22, respectively [29]. For that it creates for each network component (here: buses, carriers, loads, generators and links) a data frame listing its static attributes and a dictionary for its time-dependent attributes. The optimization software is part of DLR's Probabilistic Forecast Evaluation Tool 'ProPower' following closely the PyPSA formulation. It uses the Python-based optimization modeling language Linopy [23]. The enveloping algorithm used is the following:

Algorithm 1 Optimization of Power Flow

Input

Input for network parameters: Buses -, links-, loads-, generators attributes
ECMWF Ensemble Forecasts
ERA5 Reanalysis Observations
List of months
List of wind parks

Output

.csv-files of wind park independent data:
(Continuously Ranked Probability Score (CRPS), Root Mean Squared Error (RMSE), mean costs, mean observation, total load, total curtailment)
.csv-files of wind park dependent data:
(day-ahead schedule, balancing, forecasted wind power, observed wind power, curtailment, load shedding)

```
for month in months do
    Get list of days in corresponding month
    for day in days do
        for wp in windparks do
            Read (ensemble) forecast for each wind park and store them in data frame
            Read observation data for each wind park and store them in data frame
        end for
        Initialize networks and return conventional and stochastic network model
        Calculate network independent data
        for nw in [conventional network, stochastic network] do
            Clear day-ahead- and balancing market
            Calculate Curtailment
            Calculate RMSE and CRPS
            Calculate system costs
        end for
    end for
    Export data to .csv files
end for
```

Read Forecasts and Observation

The ensemble forecast consisting of 50 members was retrieved from ECMWF for each bus with an hourly resolution [17]. Using a power-curve the wind speed at 100 m height input data was transformed into available wind power and normalized using the nominal capacity of the wind park. The entire ensemble was used as input for the stochastic model, while only one member picked at random was used as the deterministic forecast of the conventional dispatch model. ERA5 Reanalysis data was taken as the observed wind speeds at a 100 m height and available wind power, which is required to calculate necessary balancing. The skill of the forecasts was evaluated using the RMSE for the deterministic - and the CRPS for the stochastic case (see Appendix).

Initialize Network

First, the network had to be initialized using the in section 3.1 mentioned components and their attributes as well as the respective forecasts and observations. The day-ahead market and balancing is cleared each day. It results in a Linopy model with 24 hourly timestamps also called snapshots, 13 generators, 5 links and a load time series for each of the 5 buses and 3 sectors. Further, it considers operational constraints. Namely, the flexibility and capacity bounds of the generators and links as well as the nodal balance equation.

Clear Markets

The day-ahead market and subsequently balancing is cleared for both the stochastic and the conventional model. This was done using the following algorithm:

Algorithm 2 Clearing of Markets

Input
Initialized network
Output
.csv-file of day-ahead schedule
.csv-file of balancing actions
.csv-file of required link capacity
.csv-file of load shedding

if day-ahead = conventional **then**
function PREPARE CONVENTIONAL DAY-AHEAD:
Implement nodal-balancing constraint for each bus, time stamp and member
Implement technical constraints of generators for expected dispatch
Implement technical constraints of links for expected power flow
Define conventional cost function
end function
Solve optimization problem
end if
if day-ahead = stochastic **then**
function PREPARE STOCHASTIC DAY-AHEAD:
Implement nodal-balancing constraint including expected balancing actions
Implement technical constraints of generators for expected dispatch
Implement technical constraints of links for expected power flow
Limit overall balancing to available flexibility
Limit generation after balancing to ensemble member taken as observation
Limit repurchasing of electricity to day-ahead schedule
Limit shedding to be between 0 and dispatched energy
Define stochastic cost function
end function
Solve optimization problem
end if
Export day-ahead schedule as .csv-file

Clear Balancing Market:
function PREPARE BALANCING MARKET:
Implement nodal-balancing for balancing actions
Limit overall balancing to available flexibility
Limit generation after balancing to observation
Limit repurchasing of electricity to day-ahead schedule
Limit shedding to be between 0 and dispatched energy
Define balancing cost function
end function
Solve optimization problem

Export balancing measures, link capacities and shedding results as .csv-files

Calculate System Parameter

The model performance is evaluated using further system parameters. The curtailment was calculated as the difference between the available energy production, which is the product of the observed wind power and the nominal capacity of the generators, and the actual dispatched energy. Further, the costs for the day-ahead schedule, balancing and the entire market chain as well as the RMSE and CRPS were calculated and exported as a .csv-file.

4 Results

The aim of the analysis of both dispatch models is to understand how implemented uncertainty information impact the model performance. They have been compared using system costs differentiated in day-ahead- and balancing costs, shedding and curtailment and their relation with total system costs and quality of forecast is investigated. Further, the effect of the grid design in particular of level and spatial distribution of generator flexibility and link capacity is explored.

4.1 Comparison of Conventional and Stochastic Dispatch Model

System Costs

The main goal of optimizing the energy dispatch is to minimize the operational costs under consideration of the system constraints while ensuring that the energy demand is met at all times. Hence, the comparison of system costs is essential to evaluate model performance (Fig. 3). Overall, the stochastic model reduces the average price per MWh for the total system by 0.34€ from 2.72€/MWh by the conventional model to a price of 2.38€/MWh. Considering the total load of ca. 140×10^6 MWh this amounts to a total cost reduction of around 47.5 Mio € per year.

More specifically, the system costs can be differentiated in day-ahead costs and balancing costs. In the day-ahead market the average price per MWh for the stochastic model is 2.58€/MWh, while the conventional model is cheaper at 2.29€/MWh. This is as expected as the stochastic model takes future balancing costs into account, while the conventional model optimizes the energy dispatch only considering the day-ahead market. In total, the stochastic day-ahead market is 39.6 Mio€ more expensive. The positive effect of considering expected balancing costs can be seen when comparing the average price per MWh during balancing. In case of the stochastic model it is -0.20€/MWh, while for the conventional model it is 0.43€/MWh. Considering the total load needed for balancing, the balancing costs of the conventional model are 87.5 Mio€ more expensive than the stochastic model. The difference in balancing costs can be split into two contributing factors, generator flexibility and shedding, where the generator flexibility makes up 45.7% of the difference in costs and shedding measures the remaining 54.3%.

When analyzing the balancing costs plot, one can notice the spikes in price up to 17.16€/MWh of the conventional model, which are not apparent in the stochastic model.

This indicates the use of shedding, which is with a price range from 250€/MWh to 150€/MWh the most expensive balancing measure.

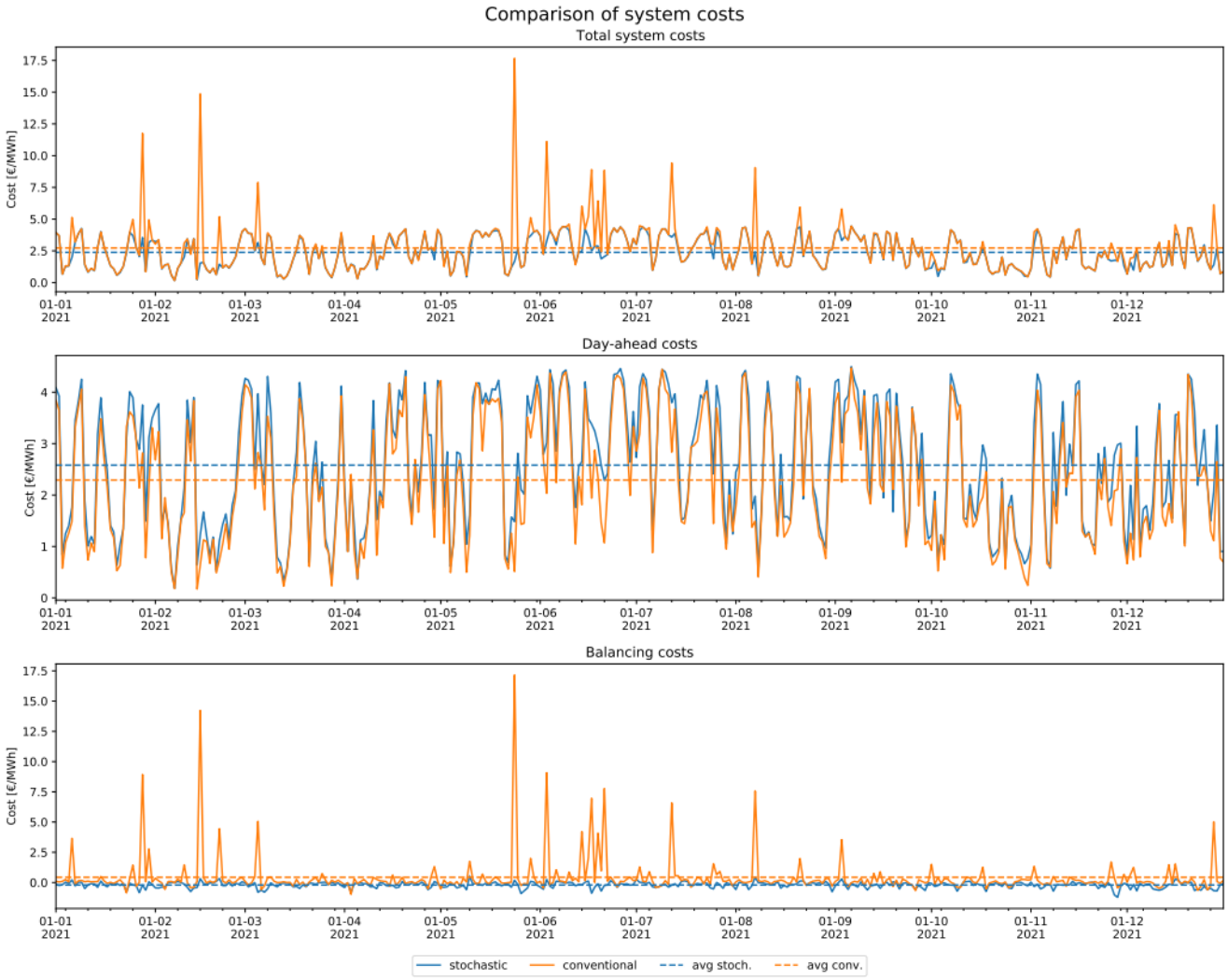

Figure 3: Comparison of system costs in 2021. Orange: conv. model, blue: stoch. model, dashed line style: average costs. Top to bottom: 1) Total system costs, 2) Day-Ahead market costs, 3) Balancing costs.

The effect of shedding on the total system costs can be nicely seen in Fig. 4. In the stochastic case there exists a limit of 4.45€/MWh for total system costs, whereas the conventional model goes up to 17.67€/MWh. Generally, it can be seen that the higher the observed wind power, the lower the system costs as the marginal cost of on- and offshore wind parks is 0€/MWh. The day with the maximal stochastic total system costs coincides with a day with very low observed wind power of only 4% of the system capacities. This indicates that the majority of the demand was covered by the OCGT generators with a marginal price of 4.50€/MWh and hence, explains the upper bound of stochastic total system cost.

Figure 4: Comparison of total system costs in 2021 for conventional and stochastic dispatch. Size of points is proportional to obs. wind power given as avg. utilization of wind park capacity (e.g. if obs. wind power is 50% all wind parks have an avg. utilization of 50% of their nom. capacity)

Curtailment

Curtailment is the deliberate suspension of (wind) power generation to balance electricity supply in case of an excess electricity supply on the grid. It is defined as the difference of observed available maximal wind power and actual dispatch of the wind parks. Due to their marginal costs of 0€/MWh it is of great advantage to minimize the share of curtailed wind energy.

The curtailment is differentiated by wind park and summarized in Table 4. The wind park with the highest amount of shedding (offshore Ems, offshore Büttel, onwind Wilhelmshaven) are all buses, where the available onshore wind power alone is a multiple of the local demand. Hence, the energy cannot alone be used to cover the local load but needs to be transported to other buses. The limiting factor here are the link capacities, which e.g. in the case of Whv-Ems and Büttel-HH are bottlenecks. The impact of link capacity on curtailment is further investigated in section 4.3.

Bus	Carrier	Model	Tot. Curtailment [MWh]	Rel. Curt. [%]
Ems	offshore	conv.	84.7040×10^5	27.3
		stoch.	84.8816×10^5	27.3
	onshore	conv.	0.4235×10^5	0.6
		stoch.	0.1105×10^5	0.2
Büttel	offshore	conv.	61.2630×10^5	32.5
		stoch.	63.2603×10^5	33.6
	onshore	conv.	6.0075×10^5	9.8
		stoch.	0.3986×10^5	0.6
Whv	offshore	conv.	1.1074×10^5	7.8
		stoch.	10.4421×10^5	72.1
	onshore	conv.	30.9758×10^5	50.4
		stoch.	21.3451×10^5	34.7
HH	onshore	conv.	0.0052×10^5	0.3
		stoch.	0.0	0.0
Ruhr	onshore	conv.	0.0	0.0
		stoch.	0.0	0.0

Table 4: Overview of total curtailment per year depending on wind park. From bus with most shedding to bus (top) to bus with lowest shedding (bottom).

Comparing curtailment in both models in Fig. 5, one notices that both show high levels of curtailment (conv.: orange area, stoch.: blue line - left y-axis) of on average 22.7% of total available wind power, but only very slight differences (green line, right y-axis) between the stochastic and the conventional model can be noticed. In total, 184.4×10^5 MWh in case of the conventional model and 184.0×10^5 MWh in case of the stochastic model were curtailed. Seasonal variations can be seen in observed wind power and correspondingly, curtailed wind energy is decreasing towards the summer.

In order to investigate the relation between difference in curtailment, observed wind power and share of curtailed energy, the same data was plotted as a scatter plot in Fig. 6. It can be seen that 1) the higher the observed wind power, the higher the curtailed energy and 2) that differences are more frequent and more pronounced in the lower two thirds of observed wind power. This can be explained considering 1) that the more wind is available, the higher the chance is that it partly has to be curtailed as the transmission links will overload and 2) that at very high observed wind power and correspondingly curtailment levels, the transmission links will most likely run consistently at nominal capacity leaving little leeway for differences between the models.

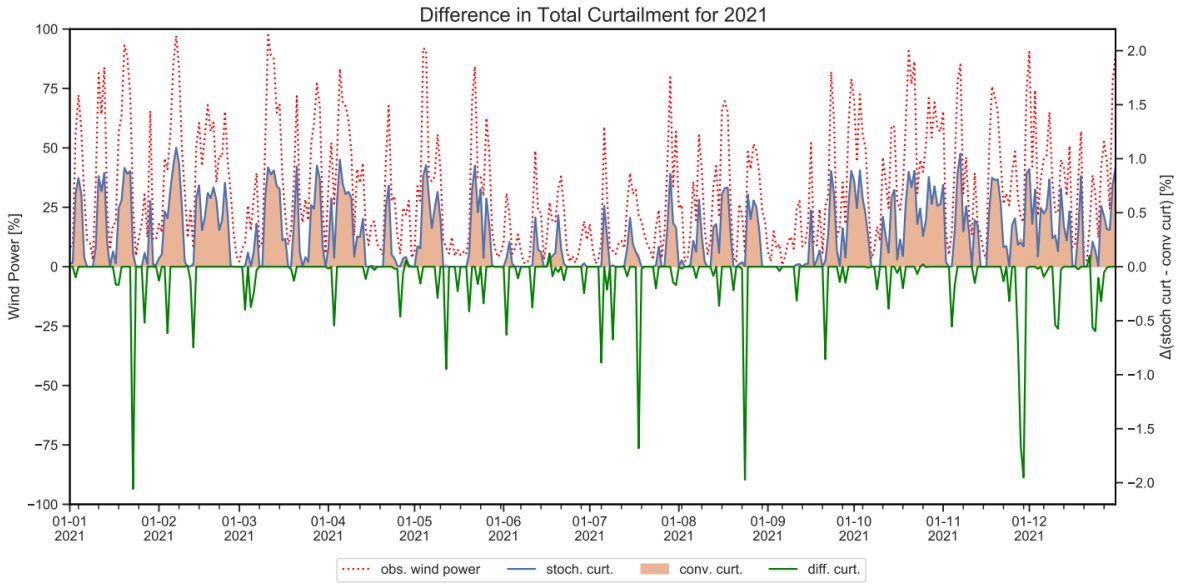

Figure 5: Comparison of daily curtailment in 2021. Left y-axis: Obs. wind power (red dotted line), stoch. curtailment (blue line), conv. curtailment (orange area). Right y-axis: Difference (stoch. - curt.) in curtailment between models (green line).

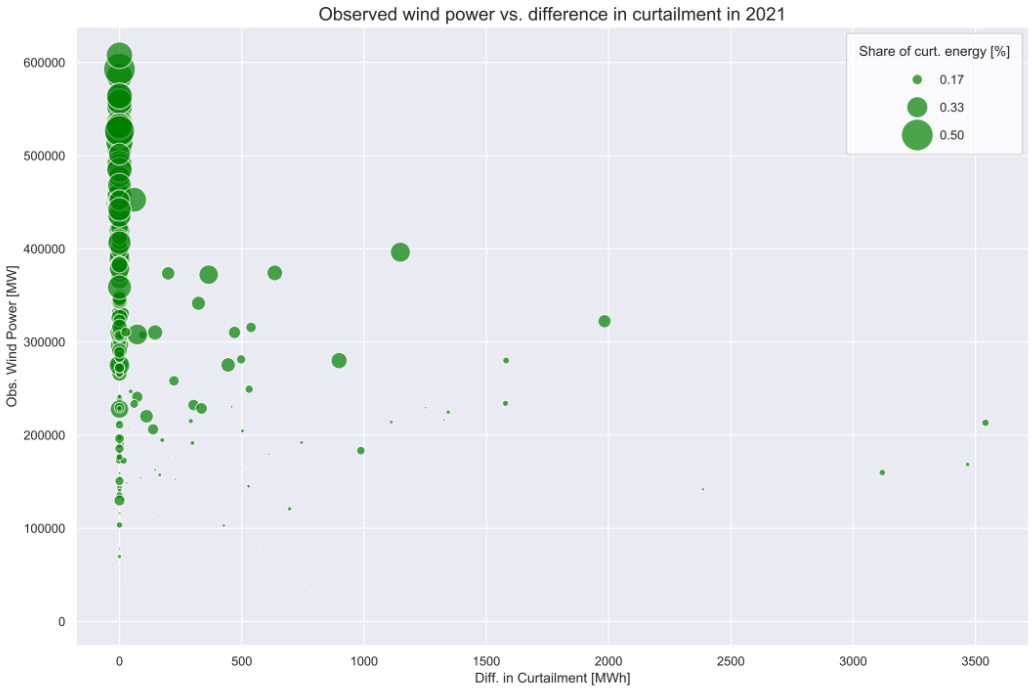

Figure 6: Total observed wind power per day summed over all wind parks vs. difference in curtailment between stochastic and conventional model in 2021. Size of points is proportional to share of curtailed energy from tot. available wind power.

Shedding

Shedding is the temporarily cutting off of electricity supply to some consumers to maintain the stability of the power grid during high demand or low supply periods. It is the most expensive balancing measure. Thus, as already shown the amount of shedded load has a significant impact on the total system costs. The two models show large differences in behavior (Fig. 7).

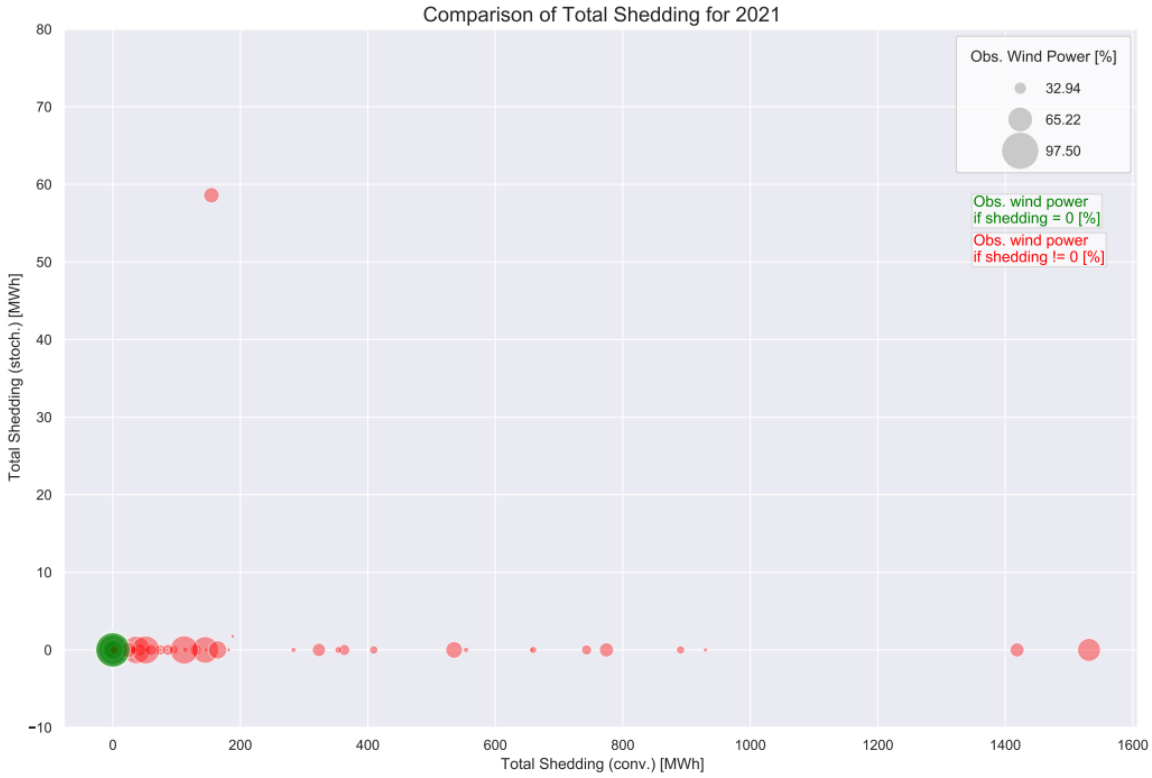

Figure 7: Comparison of total amount of shedding in 2021 between conventional and stochastic model. Red dots: Stochastic tot. system costs > conventional tot. system costs, green dots: Stochastic tot. system costs < conventional tot. system costs. Size of dots is proportional to observed wind power.

Analyzing the shedding events (red dots, Fig. 7), one can observe that the frequency and magnitude of shedding in the conventional model is much higher than in the stochastic model. In the conventional case a total of 318034 MWh (0.228% of total yearly load) is shedded compared to only 1448 MWh (0.001%) in the stochastic model.
The difference can be also quantified using the Loss of Load Expectation (LOLE) (see Appendix), which is a common measure for the security of supply and describes the statistically expected number of hours per year in which the demand will not be fully covered. For the stochastic model, LOLE is 5 hours, whereas it is 392 hours for the conventional model.

Analysis of day with highest shedding

In order to understand the difference in model behavior, the day with the highest conventional shedding event, 15.02.2021, of on average 1531 MW per hour was analyzed in more detail. On the same day no stochastic shedding occurs, making it an interesting example to compare the models. As the implemented load profiles only exhibit regular daily- and small seasonal variation a sudden spike in demand as a reason for shedding can be excluded. Hence, possible sources include very inaccurate deterministic wind power forecasts resulting in disadvantageous day-ahead schedule and the overload of link capacities disabling the transmission of energy to buses, where it is needed.

First, the accuracy of the forecast as a potential source of the shedding event was analyzed (Fig. 8).

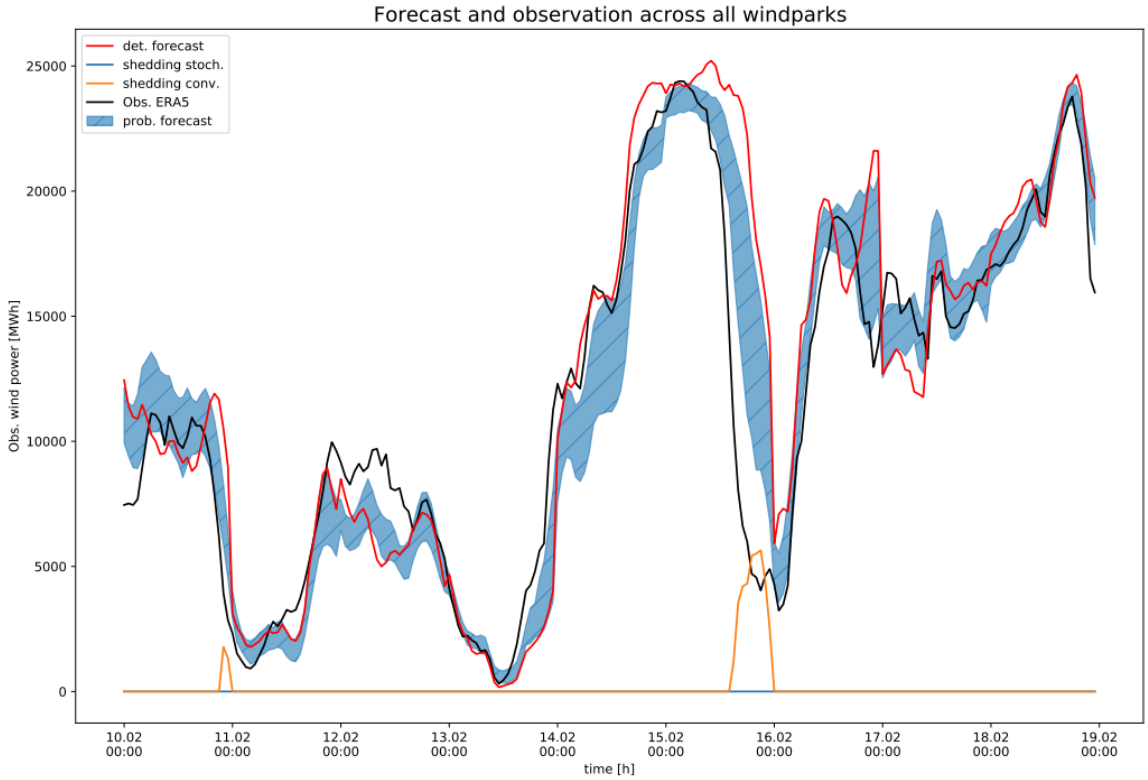

Figure 8: Forecast and observation summed up over all wind parks on 15.02.2021. Shows deterministic forecast (red line) and probabilistic forecast (blue area: 25- to 75- quantile) to ERA5 observation (black line) as well as shedding in conventional model (orange line) and in stochastic model (blue line).

The shedding event in the conventional model (orange line) can be observed in the afternoon of the 15th of February. Simultaneously, a deviation between the deterministic forecast (red line) and the ERA5 observation (black line) of roughly 19500 MWh in predicted wind power occurs. The probabilistic forecast (blue area) being in between the two other ones

predicts more accurately the severe downward ramp slightly earlier and matched better the observation.

As shedding is bus-specific, the next step of the analysis was to investigate individual nodes. For this the bus with the shedding event was identified to be Ruhrgebiet. Ruhrgebiet has by far highest demand and often relies on energy transported from Ems or Hamburg. Fig. 9 shows the bus Ruhrgebiet and again a deviation between deterministic forecast and ERA5 observation can be observed, while the probabilistic forecast matches the observation better and predicts the decrease in available wind power in the afternoon earlier. The time of the deviation corresponds to the onset of the shedding event. What happens in detail is analyzed when looking at the day-ahead schedule and dispatch as shown in Fig. 10.

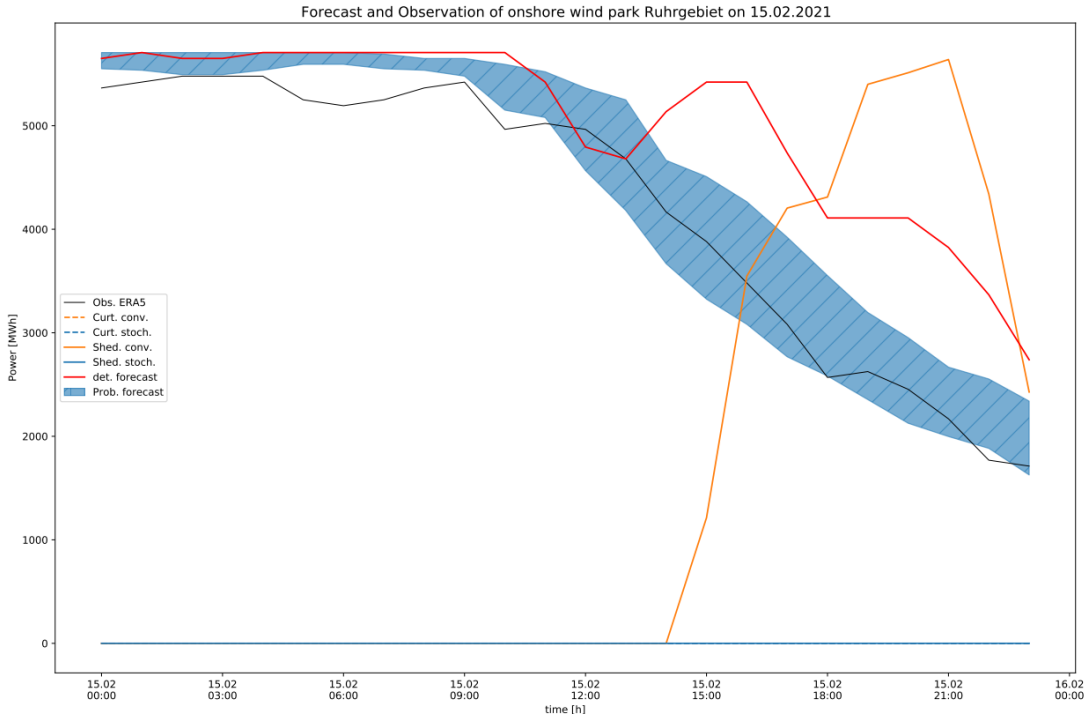

Figure 9: Forecast and observation of onshore wind park in Ruhrgebiet on 15.02.2021. Deterministic forecast (red line) and probabilistic forecast (blue area: 25-to 75-quantile) to ERA5 observation (black line), shedding in conventional model (orange line) and in stochastic model (blue line).

Generally, in Fig. 10 the conventional model is displayed by thin lines and the stochastic model by thick lines and only the OCGT is displayed as the generator most of interest. It has the highest nominal capacity $\overline{G}_{\mathrm{n,s}}$ out of all generators and is - as a conventional generator unlike the wind parks - bounded by its flexibility availability. Hence, it relies on an accurate day-ahead schedule for an efficient operation. Comparing the day-ahead schedules (green dotted line) of the two models, one notices that the stochastic model planned for a significantly higher energy generation from the OCGT generator than the conventional model in the afternoon. Combined with the flexibility to increase generation even more during balancing, it allows for producing additional 14947 MWh from the OCGT in the

afternoon (green area), which is used to avoid shedding. Nevertheless, the energy surplus produced in the stochastic model compared to the conventional one at the Ruhrgebiet bus, does not fully cover the amount of shedded load of 36989 MWh and the role of the remaining buses has to be taken into account.

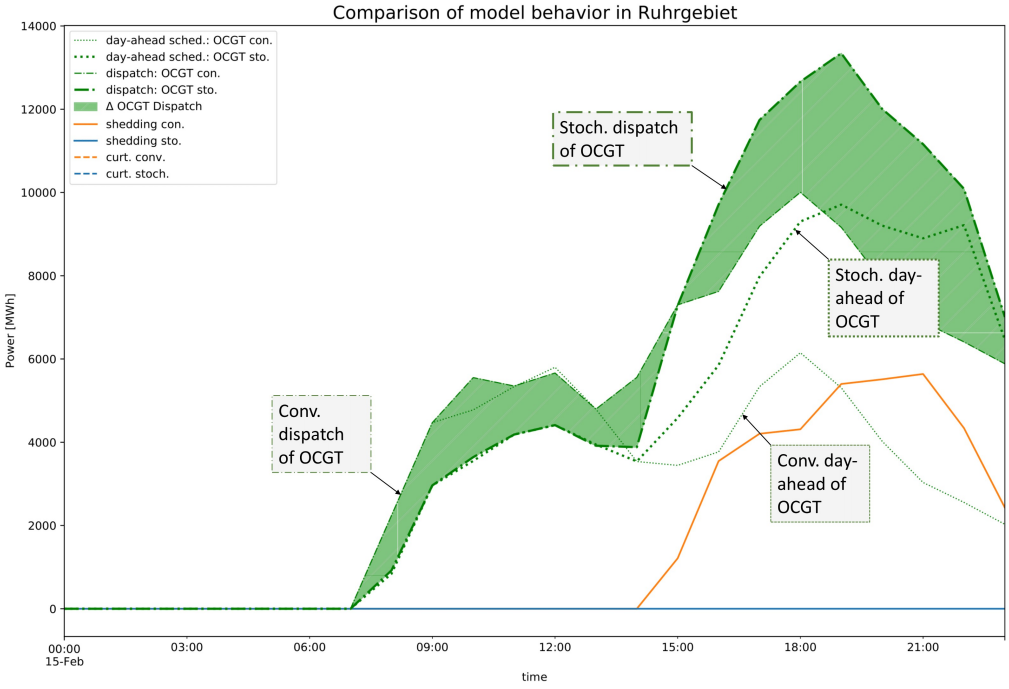

Figure 10: Comparison of model behavior on 15.02.2021 in Ruhrgebiet. Compares day-ahead schedule of OCGT (conventional: thin dotted green line, stochastic: thick dotted green line) and dispatch of OCGT (conventional: thin dash-dotted green line, stochastic: thick dash-dotted green line). Difference in dispatch is marked by green shaded area. Day-ahead schedule and dispatch of onshore wind park have been emitted for better overview.

Fig. 11 shows the probabilistic forecast at the Hamburg bus, which better predicts the decrease in available wind power towards the afternoon while the deterministic forecast overestimates wind power. As the conventional model is based only on the deterministic forecast, that predicts a high share of available wind power, no OCGT in Hamburg is scheduled (thin green dotted line, Fig. 11). On the contrary, the stochastic model schedules the OCGT at nearly nominal capacity (thick green dotted line) in the day-ahead allowing to generate a surplus of in total 22506 MWh compared to the conventional model.

For conciseness reasons, the comparison of model behaviour of the complete set of buses can be found in the appendix as the remaining buses shows only small differences between the two models. Further, the same analysis was done for the day with the second highest shedding event, the 24.05.2021, of on average 1419 MWh per hour (see Appendix).

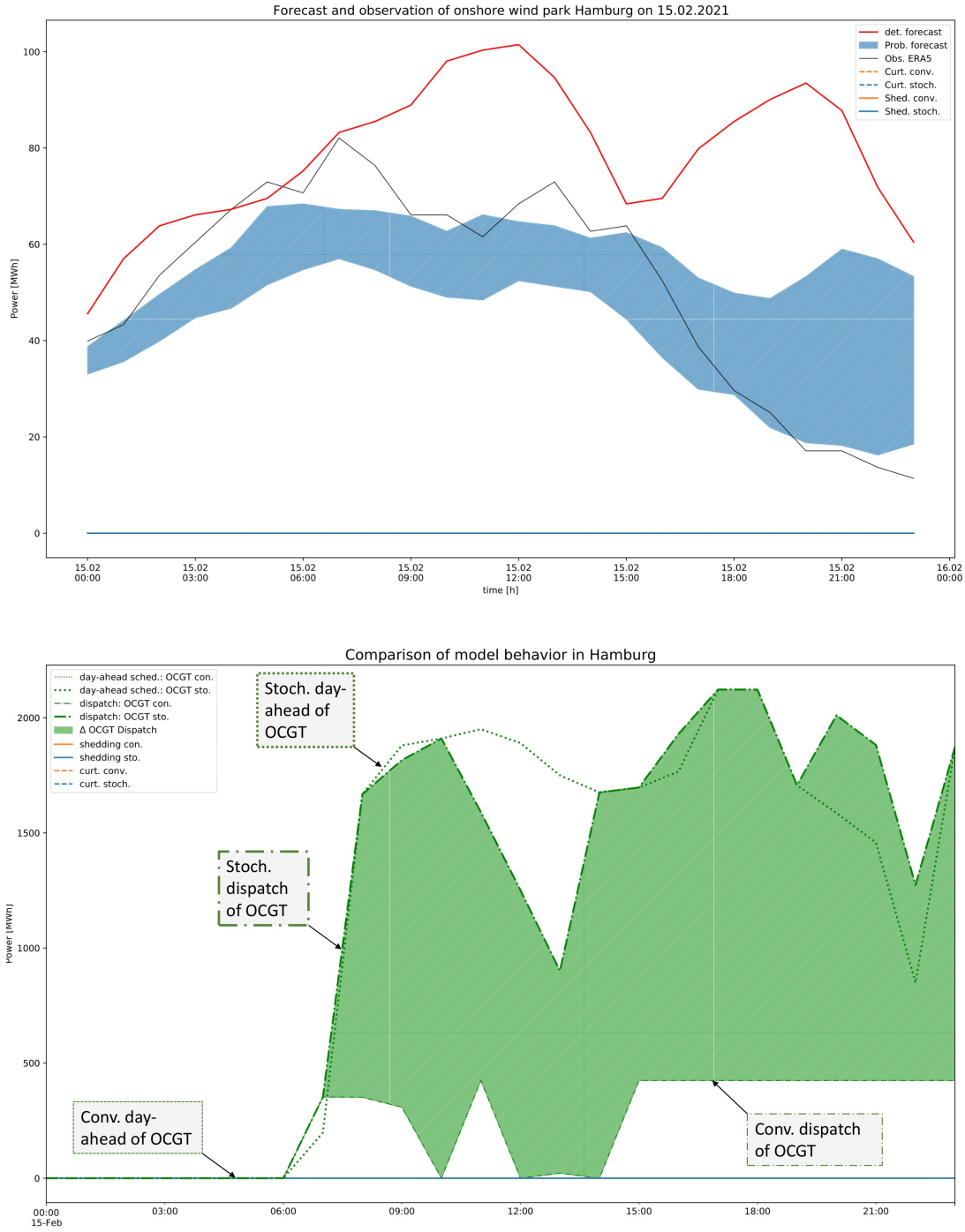

Figure 11: Analysis of model behavior in Hamburg on 15.02.2021.
Top: Forecast and observation of onshore wind park. Deterministic forecast (red line) and probabilistic forecast (blue area: 25-to 75-quantile) to ERA5 observation (black line), shedding in conv. model (orange line) and in stoch. model (blue line).
Bottom: Day-ahead schedule of OCGT (conv.: thin dotted green line, stoch.: thick dotted green line) and dispatch of OCGT (conv.: thin dash-dotted green line, stoch.: thick dash-dotted green line). Difference in dispatch: green shaded area. Day-ahead schedule and dispatch of onshore wind park have been emitted for better overview.

The additional energy produced in Hamburg was then transported to the Ruhrgebiet (orange area, Fig. 12). Partly, the nominal capacity of $\overline{G}_{\mathrm{n,s}} = 6106$ MW is reached. If the transmission is positive, the energy is transported from the first mentioned bus to the second one and if negative, vice versa. For the remaining links no significant differences between the models can be observed. Coinciding with the decrease in available wind power at roughly 3 pm, Büttel-Hamburg (blue) decrease in transmission to nearly 0 MWh, Hamburg-Ems (green) remains at full nominal capacity of 2539 MW delivering energy from Ems to Hamburg, Ems-Ruhrgebiet (red) first decreases in the afternoon and switches direction such that energy is transported from Ruhrgebiet to Ems, while Ems-Wilhelmshaven (purple) very slightly decreased after remaining constant at its nominal capacity of 428 MW. As the load of Ems is comparatively low, the energy supplied by Ruhrgebiet and Wilhelmshaven in the afternoon exceeds the local demand. Hence, it has to be transported to Hamburg to cover the load there and partly be further transported to the Ruhrgebiet via the Hamburg-Ruhrgebiet link. That Ruhrgebiet delivers energy to Ems while simultaneously shedding load suggests a tendency of the solution algorithm to push variables to their boundaries (either 0 or here total load). Hence, as the total amount of shedded load exceeds the load in other buses, it prefers to shed the entire amount in Ruhrgebiet than distributing it on multiple buses. As these tendencies are not found in the reality, it can either be avoided by adding noise to the marginal costs or by considering transmission losses of the links.

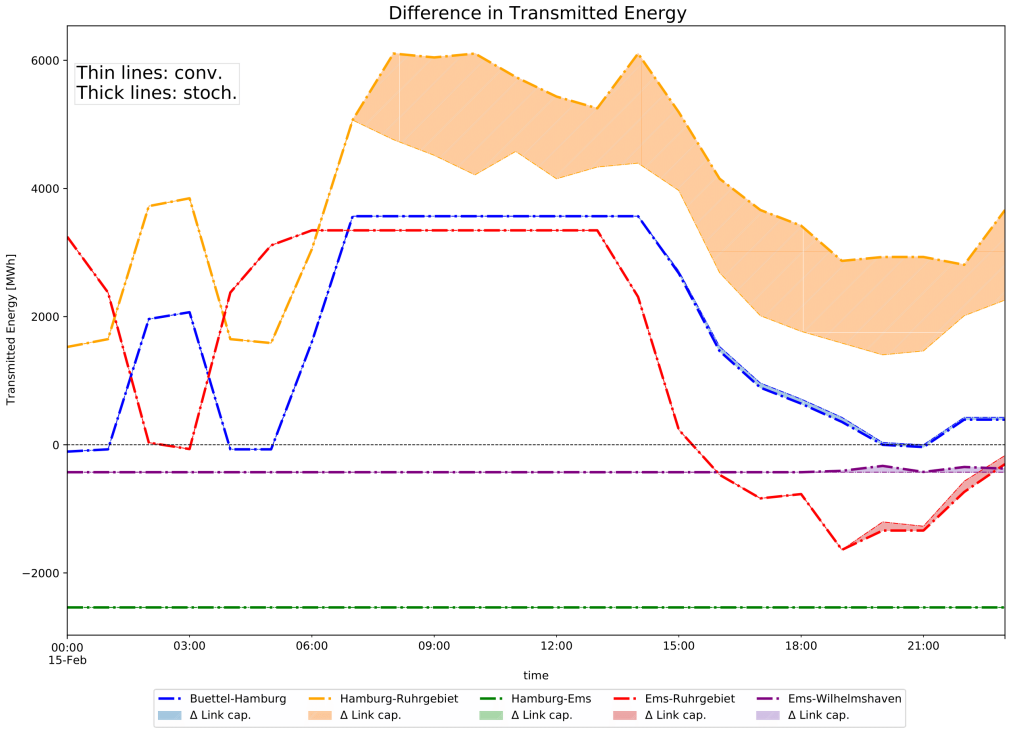

Figure 12: Comparison of link transmissions on 15.02.2021. Conv. model: thick dash-dotted lines, stoch. model: thin dash-dotted lines. Difference in transmission per link: shaded area in color corresponding to link.

Impact of Shedding and Curtailment on System Costs

The impact of shedding and curtailment on system costs is visualized in Fig. 13. The green bubbles mark days, where the conventional model was more expensive, whereas the red bubbles mark that the stochastic model was more expensive. Here, a different scaling was chosen in order to make them visible. Overall, in case of a more expensive stochastic model, the cost difference is marginal. Interestingly, this was always the case in the conventional model when no shedding took place. Further, on the same days an inverse relationship between curtailment levels and difference in costs can be observed. This suggests that in case of an accurate day-ahead schedule with no unexpected deviations as discussed in the previous chapter the conventional model yields slightly better results, while the stochastic model's day-ahead schedule tends to be less accurate as it has due to a certain amount of spread in the forecast that needs to be considered. Nevertheless, this is overshot by the inaccurate planning on days with shedding events. These are days, where both high generator flexibility and shedding costs especially in the conventional model occur as shedding only takes places once generator flexibility is insufficient to balance out missing wind power. Since the higher the shedding, the higher the difference in costs with the conventional one being more expensive and the maximum difference being 16.00€ coinciding with the day with the second highest amount of shedding of 1419 MWh. The highest stochastic shedding event of 59 MWh is the 10.05.2021. Nevertheless, the stochastic model remains slightly cheaper as simultaneously 155 MWh are shedded in the conventional model.

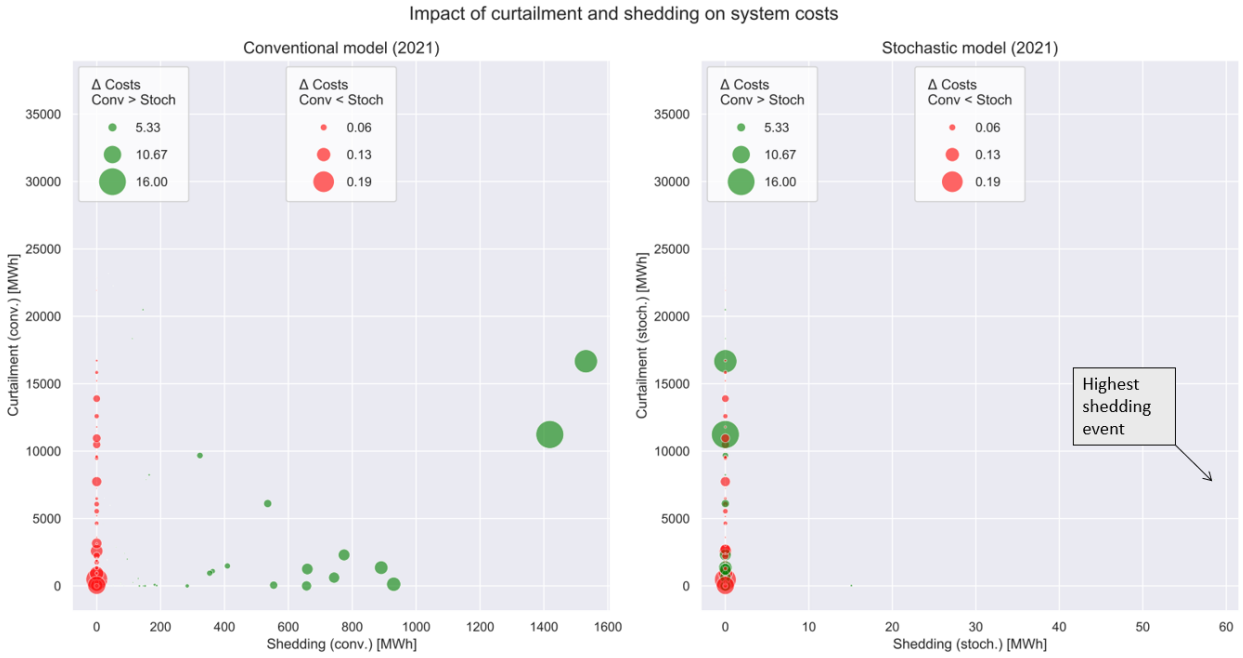

Figure 13: Comparison of impact of shedding and curtailment on total system costs between conventional model (left) and stochastic model (right). Red dots: Stochastic tot. system costs > conventional tot. system costs, green dots: Stochastic tot. system costs < conventional tot. system costs. Size of dots is proportional to difference in tot. system costs.

CRPS and RMSE

The relation between quality of forecast, observed wind power and model performance quantified in form of system costs is compared in Fig. 14. While the RMSE and CRPS cannot be compared directly, a higher score in both measures mark a higher deviation between forecast and observation. Both scores are normed with the total observed wind power per day in order to counter the effect, that the CRPS increases proportional to the observed wind power (see Appendix for formula).

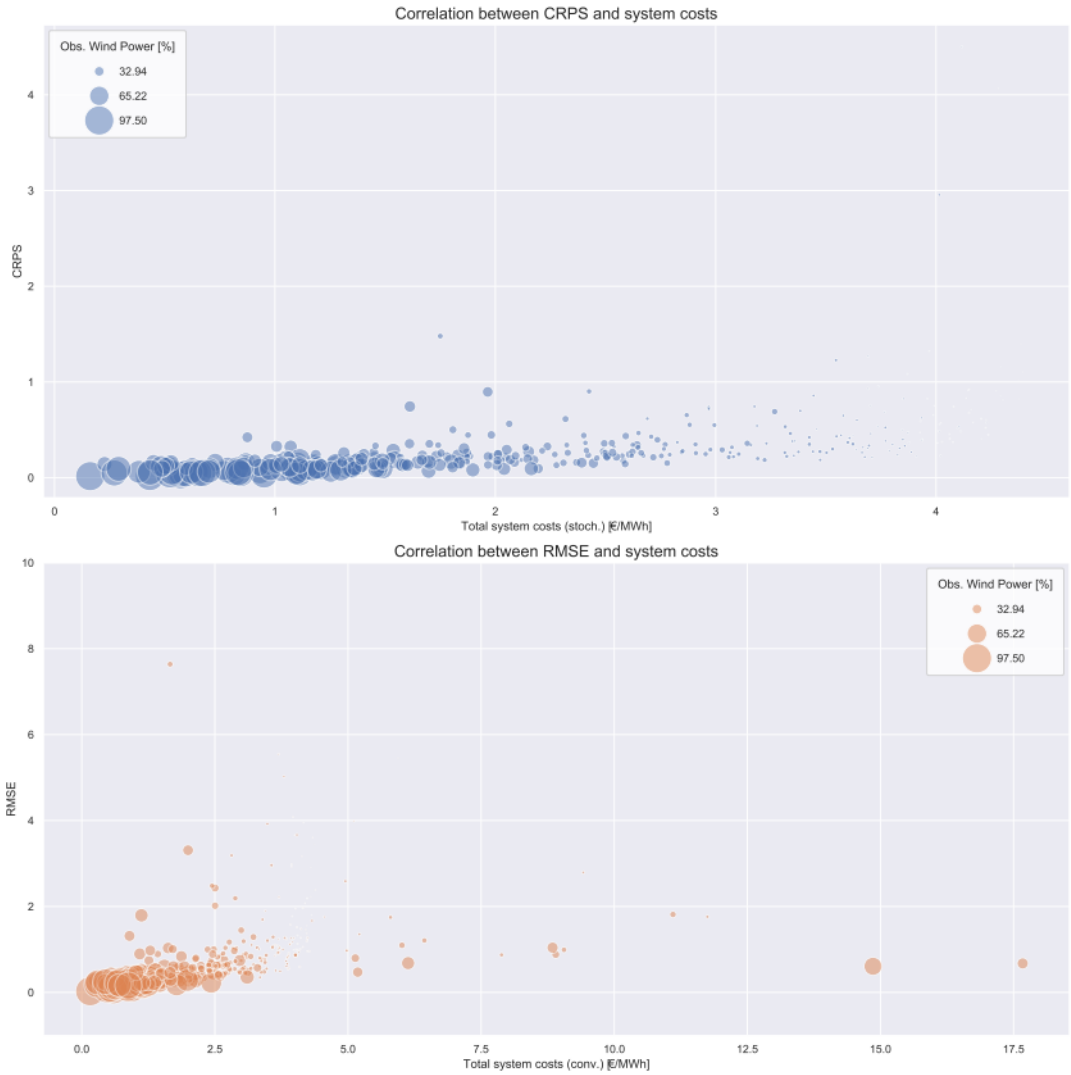

Figure 14: Comparison of correlation between quality of forecasts and total system costs. Top: CRPS vs. total system costs. Bottom: RMSE vs. total system costs. Size of dots is proportional to observed wind power. Cost axis has different scaling in plots.

In case of the stochastic model an increase in the CRPS corresponding to an increase in system costs can be observed meaning that a lower quality of forecasts results in higher

system costs. Further, the probabilistic forecast is more accurate in predicting high wind speeds than low ones. The RMSE shows a slightly different behavior. Up to system costs of 4.50€/MWh it strongly resembles the CRPS: It increases with decreased observed wind power resulting in higher system costs. This corresponds to days where small amounts of wind power is available and the great majority of the load is covered by OCGT generators. For system costs above 4.50€/MWh no clear correlation between RMSE, observed wind power and system costs can be observed. As shown before these are the days, where shedding takes place. This indicates that an inaccurate forecast cannot be considered per se as a reason for shedding. Taking the nature of the inaccuracy of forecasts in the shedding events analyzed so far into account, it suggests that rather it is decisive is to have a overly positive prediction of available wind power across the wind parks at the same time. The RMSE does not differentiate between an over- or underestimate of wind power, and by being averaged over a day tends to undervalue the occurred inaccuracy of forecast in a shedding event. Hence, it does not show a conclusive relation.

4.2 Impact of Grid Flexibility

In the second part of the thesis the impact of provided flexibility by OCGT generators on shedding and curtailment level is investigated. First, the overall level of grid flexibility are varied using the previous configuration as a reference scenario. Second, the impact of the distribution of flexibility are analyzed by comparing a scenario with the majority of the flexibility contributed by one very flexible generator to a scenario with the same amount of flexibility in MW but more evenly distributed.

Level of Flexibility

The three scenarios summarized in Table 5 are compared with the reference scenario representing a 'Medium' scenario.

Scenario	Flex. up [%]	Flex. down [%]	Tot. flex. up [MW]	Tot. flex. down [MW]
Low	15	35	3382	7891
Reference	20	40	4509	9018
High	25	45	5614	10146

Table 5: Overview of generator flexibility Levels

The model was run for each scenario using the conventional model (Fig. 15) and the stochastic model (Fig. 16). The months January to June are displayed as they show both high levels of shedding and curtailment. The results for the entire year can be found in the appendix.

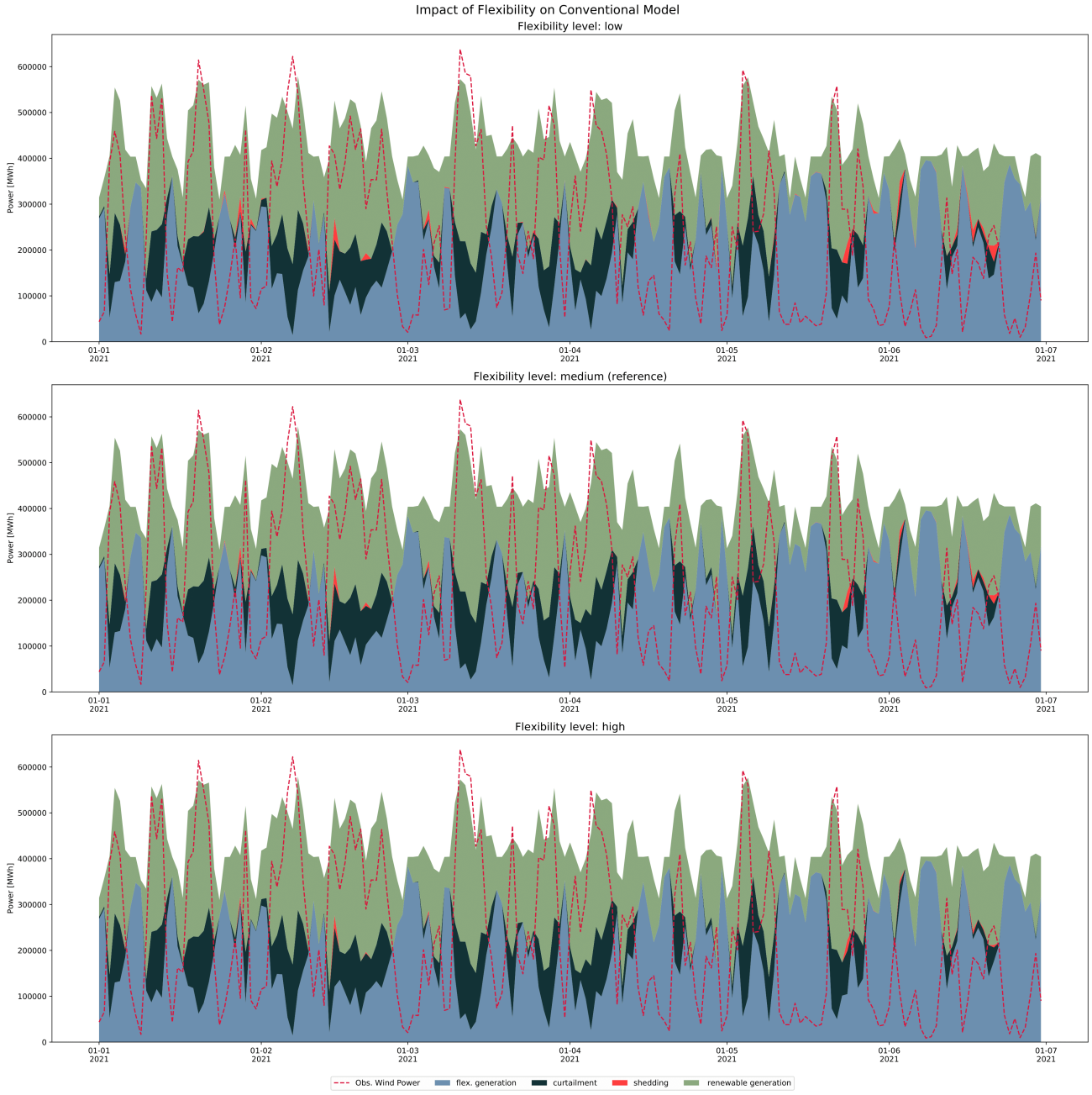

Figure 15: Daily comparison of impact of generator flexibility on the conventional model in 2021. From top to bottom: 1) Low Flexibility Scenario (FS), 2) Reference FS, 3) High FS. Generation is differentiated by flexible generator (blue) and renewable generator (green). Curtailment (black) and shedding (red), observed wind power (red dotted line) are shown.

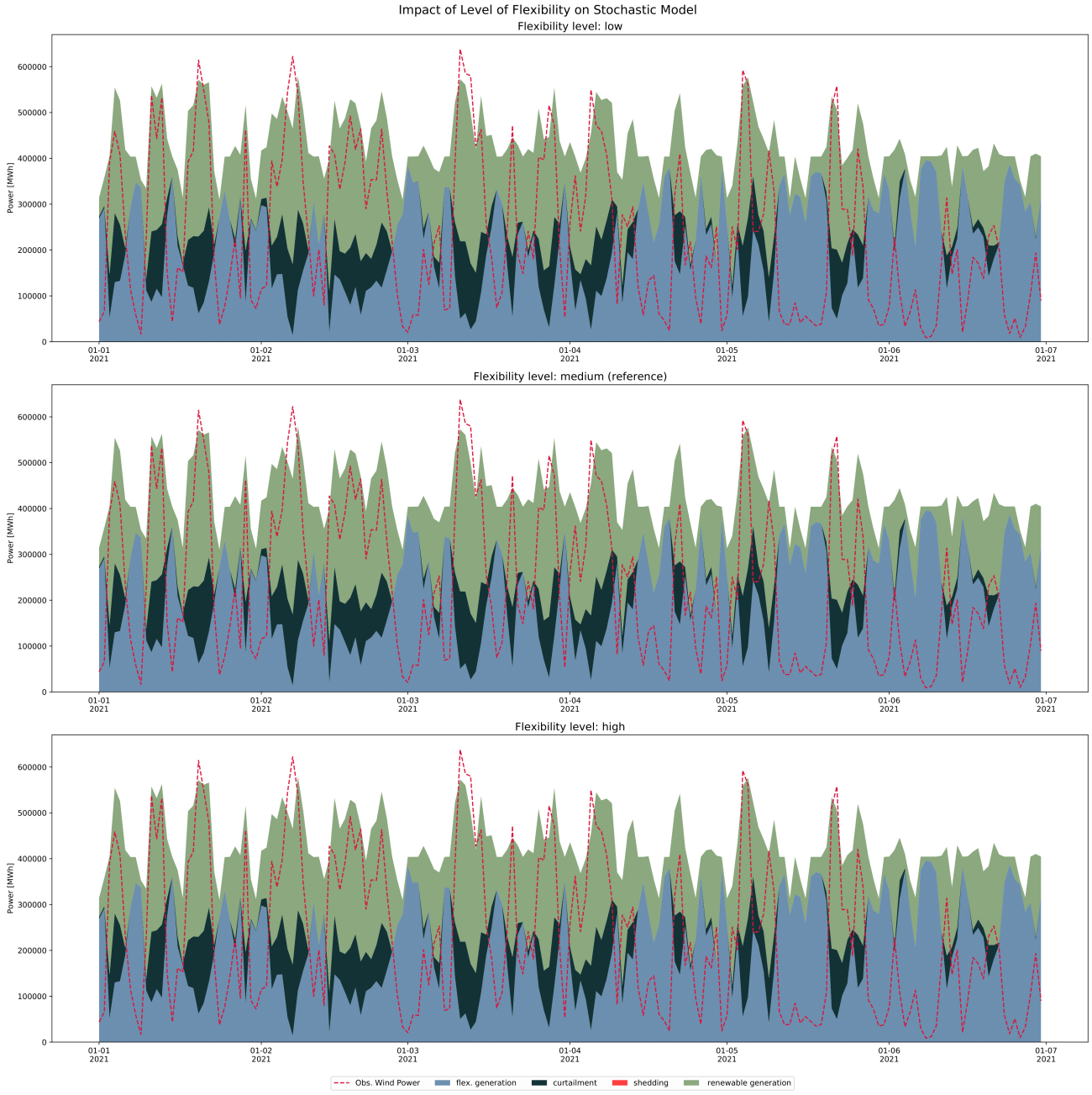

Figure 16: Daily comparison of impact of generator flexibility on the stochastic model in 2021. From top to bottom: 1) Low Flexibility Scenario (FS), 2) Reference FS, 3) High FS. Generation is differentiated by flexible generator (blue) and renewable generator (green). Curtailment (black) and shedding (red), observed wind power (red dotted line) are shown.

The amount of shedding and curtailment for the entire year was calculated for each model and flexibility level of the OCGT generators (Table 6). With increasing flexibility, the curtailment decreases slightly for the conventional model by 23780 MWh (0.1%) from scenario 'Low' to 'High' (black area, Fig. 15). Meanwhile curtailment level in the stochastic model

decreases by 8080 MWh (0.04%) from scenario 'Low' to 'Reference' to then slightly increase again with increasing flexibility (black area, Fig. 16). Overall, curtailment remains mostly stable at a high level. This suggests that curtailment rather stems from the high wind power input or restrictions in the link capacities than due to limited generator flexibility.

A strong decrease of shedding with increasing generator flexibility can be observed for both models. The conventional model reduces shedding by 0.98% (651705 MWh) from scenario 'Low' to 'High' (red area, Fig. 15), while no shedding (red area, Fig. 16) occurs in the stochastic model anymore for high flexibility. This supports the observations made in the analysis of a shedding event on 15.02.2021, where the conventional model performed suboptimal by its inaccurate day-ahead schedule and lacked sufficient flexibility to balance the deviations between forecast and observation.

	Model	Low [MWh]	Reference [MWh]	High [MWh]
curt.	conv.	184.6223×10^5	184.4863×10^5	184.3845×10^5
	stoch.	184.1063×10^5	184.0255×10^5	184.0258×10^5
shed.	conv.	66.6277×10^4	31.8034×10^4	1.4572×10^4
	stoch.	1.0744×10^4	0.1768×10^4	0.0

Table 6: Overview of shedding and curtailment depending on generator flexibility levels in 2021 with total yearly load of ca. 140×10^6 MWh.

Spatial Distribution of Generator Flexibility

The impact of spatial distribution of flexible generators has been investigated by comparing the two scenarios with the reference scenario (Table 7). Both configurations contribute a comparative level of flexibility (localized - up: 4828 MW, down: 8684 MW, distributed - up: 4918 MW, down: 8393 MW). The 'localized' scenario centers the provided generator flexibility on the OCGT generators in Ruhrgebiet, Hamburg and Wilhelmshaven and the 'distributed' scenario shares the flexibility among all generators. The aim of the 'localized' scenario was to focus the flexibility as much as possible on the OCGT generator in Ruhrgebiet while still avoiding infeasibilities when optimizing. The idea of the 'distributed' scenario was to distribute the provided flexibility in MW as evenly as possible between the generators. Considering the huge difference in nominal capacities of the OCGT generators, this resulted in setting the smaller generators (Büttel, Wilhelmshaven, Ems) to maximal flexibility and distributing the remaining flexibility evenly between Hamburg and Ruhrgebiet.

Scenario	Generators	Flex. up [%]	Flex. down [%]	Flex. up [MW]	Flex. down [MW]
Localized	HH	23	23	488	488
	Whv	78	78	484	484
	Ruhr	20	40	3856	7712
Distributed	Büttel	100	100	216	216
	HH	87	100	1846	2122
	Whv	100	100	621	621
	Ems	100	100	306	306
	Ruhr	10	28	1929	5398
Reference	Büttel	20	40	43	86
	HH	20	40	425	850
	Whv	20	40	124	248
	Ems	20	40	61	122
	Ruhr	20	40	3856	7712

Table 7: Overview of generator flexibility levels

The amount of shedding and curtailment for the entire year was calculated and summarized in Table 8.

	Model	Localized [MWh]	Distributed [MWh]	Reference [MWh]
curt.	conv.	184.1206×10^5	184.3204×10^5	184.4863×10^5
	stoch.	184.0255×10^5	184.2087×10^5	184.0255×10^5
shed.	conv.	29.5015×10^4	30.2883×10^4	31.8034×10^4
	stoch.	0.1201×10^4	1.8297×10^4	0.1768×10^4

Table 8: Overview of shedding and curtailment depending on flexibility distribution for a total yearly load of 140×10^6 MWh.

In general, the 'distributed' scenario shows slightly higher curtailment and shedding for both models. For the conventional model curtailment increases by 19980 MWh and shedding by 7868 MWh. For the stochastic model curtailment increases by 18320 MWh and shedding by 17096 MWh compared to the 'localized' scenario. While intuitively distributed flexibility might appear to be more reasonable, looking at the shedding of individual buses (Table 9) explains the increase in the 'distributed' scenario. One can observe that for the conventional model with distributed flexibility all buses experience less shedding except for Ruhrgebiet. But since the load in Ruhrgebiet is significantly higher than at the remaining buses, the shedding overall increases. Hence, one can conclude that not just the overall level of flexibility is important but that the provided flexibility needs to ideally coincide with the buses with high demand and correspondingly high potential for shedding. The dependency on

Model	Bus	Localized [MWh]	Distributed [MWh]	Difference [MWh]
conv.	HH	179	89	90
	Ems	367	0	367
	Whv	15109	7446	7663
	Ruhr	279359	295347	-15988
stoch.	Whv	0	1577	-1577
	Ruhr	1202	16321	-15119

Table 9: Overview of shedding depending on flexibility distribution

the location of provided flexibility can be lifted by having sufficiently high link capacity to transport energy to any bus. This will be tested in the next section. While in the stochastic model, overall shedding is lower and restricted to only Ruhrgebiet and Wilhelmshaven, the same effect of having a significant increase in shedding in Ruhrgebiet can be observed.

4.3 Impact of Link Capacity

The impact of varying link capacity on the model performance is investigated and compared to the transmission line usage in the reference scenario (Fig. 17, top). The link HH-Ruhr has the highest nominal capacity and transports the most energy from Hamburg to Ruhrgebiet. Ruhrgebiet also receives energy from Ems but the link Ems-Ruhr reaches partly its nominal capacity limit of 3567.35 MW. Hence, Ems also transports energy to the Ruhrgebiet via Hamburg using the HH-Ems link, which is permanently at its full capacity of 2538.58 MW. This could again be an artefact of the solution algorithm, which pushes the variables to their boundaries as it is physically unreasonable to transport energy to Ruhrgebiet via Hamburg from Ems, if the link Ems-Ruhr is not fully occupied. Again, this could be avoided by implementing transmission losses proportional to link lengths. The three scenarios 'Reference', 'Ems' and 'Both' (Table 10) are compared to investigate the energy transport with a focus on the bus Ruhrgebiet and its impact on shedding, curtailment and system costs.

Nom. Cap. [MW]	Reference	Ems	Both
HH-Ruhr	6105.94	3567.35	6105.94
Ems-Ruhr	3567.35	6105.94	6105.94

Table 10: Link capacities of HH-Ruhr and Ems-Ruhr for different scenarios

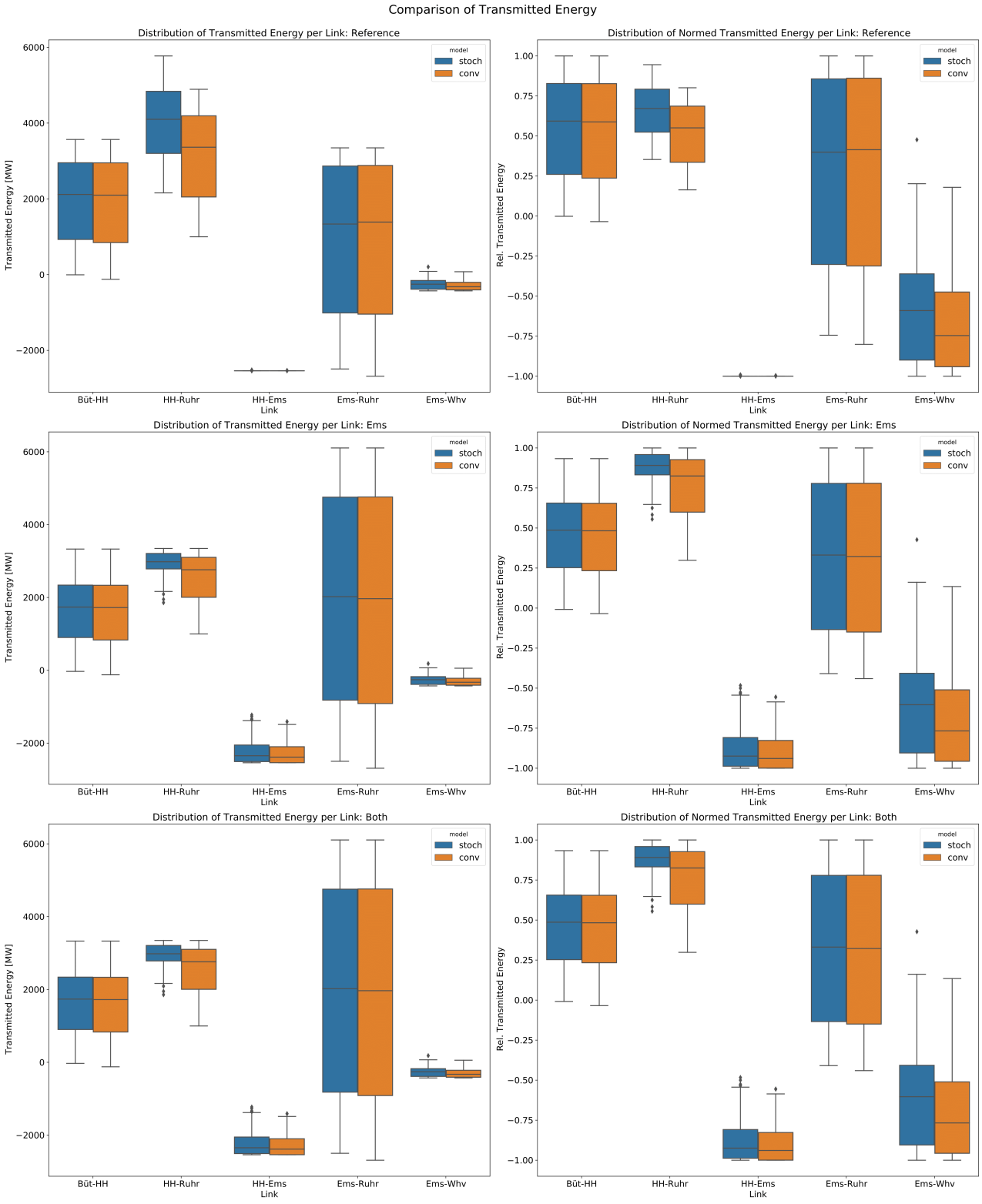

Figure 17: Distribution of transmission line usage of links in scenarios 'Reference' (top), 'Ems' (middle) and 'Both' (bottom). Conv. model: orange, stoch. model: blue. Bar plots from left to right in all plots: Büttel-Hh, HH-Ruhr, HH-Ems, Ems-Ruhr, Ems-Whv.

For scenario 'Ems' (Fig. 17, middle) the relative transmission from HH-Ruhr increases significantly due to the decrease in nominal capacity. Consequently, the energy s to Hamburg from Büttel and Ems both decrease. Instead the energy transports from Wilhelmshaven to Ems and from Ems to Ruhrgebiet increase.

For scenario 'Both' (Fig. 17, bottom) the transmission via the HH-Ruhr link increases again compared to 'Ems' to slightly below the transmission level in the 'Reference' scenario. Similarly, HH-Ems returns to running at full capacity as already in 'Reference'. The utilization Büttel-HH slightly increases compared to 'Ems', while Ems-Whv remains comparatively stable.

The average total system cost per MWh, yearly curtailment and shedding is given for each scenario in Table 11. By increasing the nominal capacity of Ems-Ruhr and decreasing the nominal capacity HH-Ruhr by the same amount in scenario 'Ems', the total amount of curtailment is reduced by 336159 MWh and 331550 MWh for the conventional and stochastic model compared to reference scenario, respectively. However, shedding increases by 131141 MWh and 1070 MWh, respectively. Overall, the total system costs increase for the conventional model from 2.72 to 2.76€/MWh and decrease from 2.38 to 2.28€/MWh for the stochastic one. Comparing 'Both' with the reference scenario similar observations can be made. Curtailment decreases by 483694 MWh for the conventional model and by 579085 MWh for the stochastic one. Shedding increases by 175669 MWh and 1483 MWh, respectively. Similarly, the total system costs also increase for the conventional model from 2.72 to 2.77€/MWh and decreases from 2.38 to 2.24€/MWh for the stochastic model. Overall, for total system costs an increasing trend in total system costs for the conventional model and a decreasing trend for the stochastic model can be observed. This is explained by the effect of curtailment and shedding. Curtailment decreases in 'Ems' and 'Both' compared to the reference scenario as in both cases, the link Ems-Ruhr doubles in nominal capacity and previously curtailed energy can be transported now to the Ruhrgebiet bus. In the reference scenario, in total 85.13×10^5 MWh in conventional and 85.00×10^5 MWh in the stochastic model are curtailed compared to only 21.73×10^5 MWh (conventional) and 21.73×10^5 MWh (stochastic) in scenario 'Both'. Hence, more wind energy with a marginal cost of 0€/MWh is utilized in both systems. For the stochastic model a proportional relationship is observed: The lower total curtailment, the lower are the total system costs as more free wind energy is used in place of the OCGTs with a marginal cost of 4.50€/MWh. Further with an increased share of wind energy in the power system the importance of an accurate forecast increases too. As shown before the probabilistic forecast more accurately predicts a sudden decrease in available wind power and hence, avoids a shedding event resulting in lower system costs compared to the conventional model. For the same reason, total system costs increase for the conventional dispatch model for lower shares of curtailment. It has been observed that during shedding events the deterministic forecast tends to overestimate available wind power, which leads to a disadvantageous day-ahead schedule. This can be seen when considering the difference in balancing costs, the share of costs stemming from shedding events increases with lower share of curtailment. In the reference scenario shedding was responsible for 54.3% of the cost difference compared to 61.4% in scenario 'Ems' and 63.1% in scenario 'Both'.

Scenario	Model	Tot. system cost [€/MWh]	Curtailment [MWh]	Shedding [MWh]
Reference	conv.	2.72	184.4864×10^5	31.8034×10^4
	stoch.	2.38	184.0255×10^5	0.1768×10^4
Ems	conv.	2.76	150.8705×10^5	44.9175×10^4
	stoch.	2.28	150.4475×10^5	0.2838×10^4
Both	conv.	2.77	136.5150×10^5	49.3703×10^4
	stoch.	2.24	126.1170×10^5	0.3251×10^4

Table 11: Comparison of system costs, curtailment and shedding for link capacity scenarios

5 Discussion and Conclusion

The increasing share of stochastic producers like wind parks in electricity grids in order to meet urgent climate goals requires an adaption of today's energy dispatch strategies based on reliable conventional producers like OCGT. This thesis discusses a stochastic model for the clearing of the day-ahead market, which - based on ensemble forecast - includes expected balancing costs when determining the optimal day-ahead schedule. The stochastic dispatch model is compared to a conventional model, which optimizes the day-ahead schedule using a least-cost merit order. Both model performances are evaluated by comparing total system costs as well as the amount of curtailment and shedding. Further, the impact of the level and spatial distribution of generator flexibility as well as of link capacities has been analyzed.

Overall, the stochastic model yields a decrease in total system costs by 0.34€/MWh from 2.72€/MWh to 2.38€/MWh equalling savings of around 47.5 Mio€ when considering total system load. While the day-ahead market is more expensive in the stochastic model than in the conventional model due to already taking potential balancing measures into account, costs for balancing measures are decreased from 0.43€/MWh for the conventional model by 0.63€/MWh to -0.20€/MWh. The cost differences in balancing between both models is caused by 54.3% due to higher shedding in the conventional dispatch model. Regarding curtailment, the stochastic model reduces the total amount of curtailed wind energy by ca. 4000 MWh from 184.4×10^5 MWh (22.8%) to 184.0×10^5 MWh (22.7%), while in shedding the difference is ca. 317000 MWh. In total, the conventional model sheds 318034 MWh of load (0.228%), while the stochastic model only sheds 1448 MWh (0.001%). An analysis of the day with the highest shedding event suggests that a sudden deviation between deterministic forecast and the observed ERA5 data across all buses can trigger a shedding event. In this case a bad conventional day-ahead schedule limits generation of OCGT generators and flexible generation is unable to ramp up to the needed level. Since the analysis of RMSE and system costs shows no clear correlation between shedding events and general quality of the deterministic forecast, it suggests that it is important that 1) the forecast strongly overestimates available wind power and 2) the sudden deviation between forecast and observation is temporarily correlated between all or most buses.

The sensitivity analysis of the impact of generator flexibility levels and spatial distri-

butions and link capacities prompted four conclusions: 1) The higher the overall generator flexibility within in the power system, the lower shedding levels occur as OCGT generators can balance out higher unexpected deviations in provided wind power. No strong effect on curtailment has been observed. 2) The most flexible generators ideally should be located at the bus with the highest load. 3) Increasing the nominal capacity of links starting at a bus with a high wind power input to buses with a high load, strongly decreases curtailment. 4) An increased share of wind energy in the power system increases the importance of having skillfull weather forecasts to avoid shedding, which benefits the stochastic dispatch model, while it worsens the performance of the conventional model due to high shedding costs resulting in increased total system costs. This shows that with an increasing share of wind energy and other stochastic energy producers, the advantage of the stochastic dispatch model is reinforced and implementing uncertainty information becomes extremely beneficial.

In general, the aim of this thesis is to understand and explore the behaviour of the stochastic model, its advantage against the conventional model and its interaction with the grid design. Thus, a rather generic, simple network is implemented, which clearly highlights the working mechanisms of the model and its dependency on grid parameters instead of being as close as possible to a real power system. Hence, it is important to note some of its limitations. The network was based on a simplified model of the power system and neglects features of real-world power systems such as transmission losses, detailed representations of different generator types, storage units, price elasticity, a large number of buses and links and flexibility-dependent marginal costs. This leads among others to (in the real world) unacceptably high shedding levels, which affect negatively the performance of the conventional model. Nevertheless, shedding was responsible for only 54.3% of the cost difference in balancing between the models in the reference scenario, which still shows that the stochastic model also reduces balancing costs that emerge from OCGT flexibility. Further, the study only considered a single day-ahead time horizon and did not account for the intraday market that is based on updated and improved forecasts.

6 Outlook

The results of this thesis suggest that utilizing uncertainty information from ensemble forecast for optimizing the energy dispatch can significantly improve the performance of the power system. The stochastic dispatch model resulted in a decrease in total system costs and reduced the amount of curtailment and shedding considerably compared to the conventional model. The analysis of the impact of generator flexibility levels, spatial flexibility distribution and link capacities provided valuable insights into the design and operation of power networks with high shares of stochastic renewable energy sources.

Future research could integrate above mentioned features for a more detailed representations of transmission networks and generator types in order to improve the realism of the model and its applicability in real-world applications. Further, different methods of implementing expected balancing costs in the optimization such as utilizing historic balancing

costs or only taking specific members of the ensemble forecast such as the median or the minimum and maximum can be tested and compared in terms of accuracy and computational complexity.

The results of this study show that with an increasing share of wind power as a representative stochastic producer, considering their intermittent nature in the electricity market by implementing uncertainty information becomes more and more beneficial to an efficient power system operation. This finding can support the design and operation of power systems with high shares of stochastic renewable energy sources, which are inevitable for a successful transition to a low-carbon future in order to meet urgent climate goals. The insights gained in this study as part of research in the field of renewable energy and power system optimization can also support political decisions related to energy dispatch and the grid integration of renewable energy source using more skillfull forecasts i.e. forecasts including uncertainty information.

7 Acknowledgments

I would like to thank my supervisor Dr. Lüder von Bremen for his guidance and support since the very first moment I started working at DLR. Likewise, I would like to thank Dr. Bruno Schyska and Hauke Bents for the numerous times their insights, hard work and continuous feedback helped me to move forward with the project. All of them created a welcoming and supportive atmosphere, which made my time at the DLR a great and inspiring experience. Further, I would like to express my gratitude to Prof. Stefan Kettemann for accompanying the thesis from the side of the university and being my second reader.

I would also like to thank my friends, in particular, those who were part of my three years at university. Thank you for making this process a lot more enjoyable and thank you for helping me grow both academically and personally. I will always be grateful for the moments I spent with you. Finally, I would like to thank my family for being my motivation and my greatest support.

Thank you,

Clara Elisabeth Buller

Statutory Declaration

Family Name, Given/First Name	Buller, Clara Elisabeth
Matriculation number	30004416
Kind of thesis	Bachelor

English: Declaration of Authorship

I hereby declare that the thesis submitted was created and written solely by myself without any external support. Any sources, direct or indirect, are marked as such. I am aware of the fact that the contents of the thesis in digital form may be revised with regard to usage of unauthorized aid as well as whether the whole or parts of it may be identified as plagiarism. I do agree my work to be entered into a database for it to be compared with existing sources, where it will remain in order to enable further comparisons with future theses. This does not grant any rights of reproduction and usage, however.

The Thesis has been written independently and has not been submitted at any other university for the conferral of a PhD degree; neither has the thesis been previously published in full.

German: Erklärung der Autorenschaft (Urheberschaft)

Ich erkläre hiermit, dass die vorliegende Arbeit ohne fremde Hilfe ausschließlich von mir erstellt und geschrieben worden ist. Jedwede verwendeten Quellen, direkter oder indirekter Art, sind als solche kenntlich gemacht worden. Mir ist die Tatsache bewusst, dass der Inhalt der Thesis in digitaler Form geprüft werden kann im Hinblick darauf, ob es sich ganz oder in Teilen um ein Plagiat handelt. Ich bin damit einverstanden, dass meine Arbeit in einer Datenbank eingegeben werden kann, um mit bereits bestehenden Quellen verglichen zu werden und dort auch verbleibt, um mit zukünftigen Arbeiten verglichen werden zu können. Dies berechtigt jedoch nicht zur Verwendung oder Vervielfältigung.

Diese Arbeit wurde in der vorliegenden Form weder einer anderen Prüfungsbehörde vorgelegt noch wurde das Gesamtdokument bisher veröffentlicht.

May 15^{th}, 2023

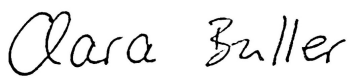

A Appendix

The sections included here serve for deeper explanations or additional information of ideas discussed in the main text.

A.1 Quality Evaluation of Forecasts

RMSE

The quality of the deterministic forecasts was evaluated using a normed root-mean-square error (RMSE), which quantifies the difference between the forecast ($F_{\mathrm{t,S}}$) and the observation ($O_{\mathrm{t,S}}$) for each generator S and time step t in a day. The difference was weighted using $p_{\mathrm{nom,S}}$. Furthermore, it was normalized using the weighted, average observed wind speed for each generator for the entire day ($\langle O \rangle_{\mathrm{t}}$).

$$RMSE = \frac{\sqrt{\langle (F_{\mathrm{t,S}} \cdot p_{\mathrm{nom,S}} - O_{\mathrm{t,S}} \cdot p_{\mathrm{nom,S}})^2 \rangle_{\mathrm{t}}}}{\langle O \rangle_{\mathrm{t}}} \tag{1-32}$$

CRPS

Subsequently, the quality of the probabilistic forecasting was quantified using a normed continuous ranked probability score (CRPS). It is a quadratic measure of the difference between the cumulative distributive function (CDF) of the ensemble forecast denoted as $\mathbf{F}_{\mathrm{t,S}}$ and the empirical CDF of the observation $\mathbb{1}(x \geq y)$ [30] with $\mathbb{1}$ being the indicator function. Mathematically, it can be expressed as:

$$CRPS = \frac{\left\langle \int \langle [\mathbf{F}_{\mathrm{s,T}} - \mathbb{1}(x \geq y)]^2 dx \right\rangle_{\mathrm{t}}}{\langle O \rangle_{\mathrm{t}}} \tag{1-33}$$

A.2 Loss of Load Expectation (LOLE)

The Loss of Load Expectation quantifies the number of years, in which it is statistically expected that supply does not cover demand and load will be shedded [31]. It can be computed as follows:

$$LOLE = \sum_{t} \mathbb{1}(g_{\mathrm{n,s,t}} + g^{+}_{\mathrm{n,s,t}} - g^{-}_{\mathrm{n,s,t}} < L_{\mathrm{n,s}} - g^{*}_{\mathrm{n,s,t}}) \tag{1-34}$$

A.3 Analysis of Shedding Event on 15.02.2021

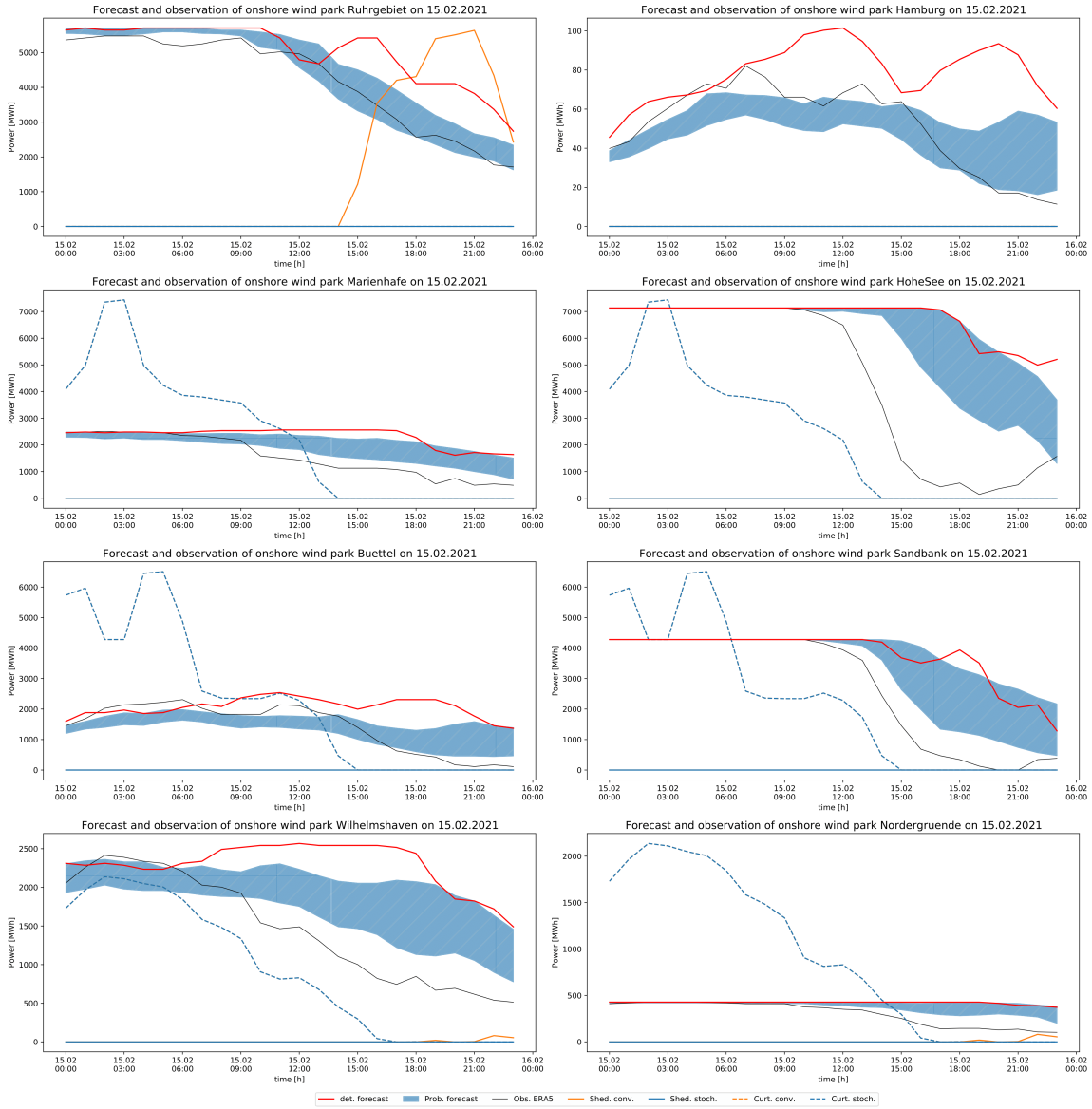

Figure 18: Comparison of forecast and observation for all buses

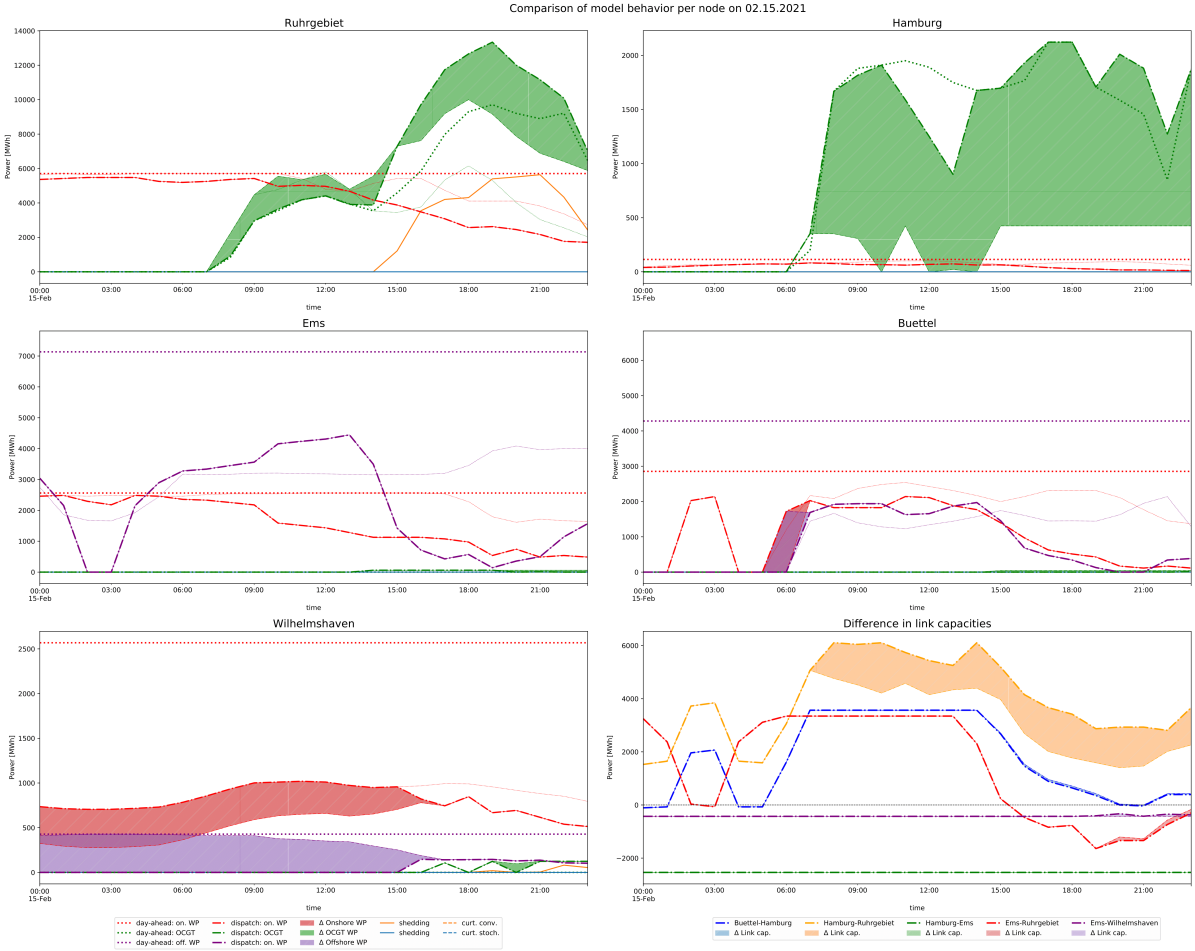

Figure 19: Comparison of model behavior for all buses

A.4 Analysis of Shedding Event on 24.05.2021

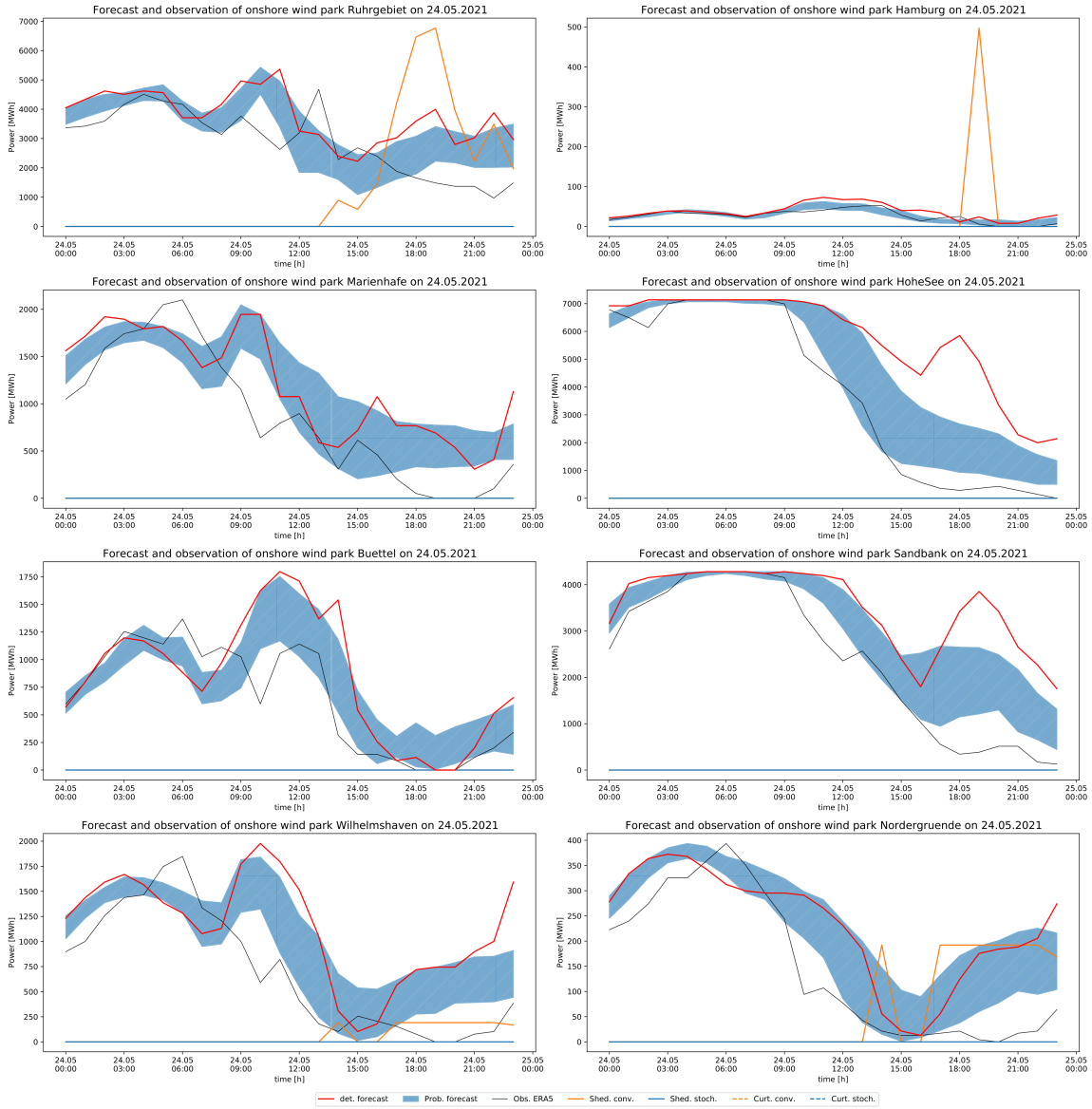

Figure 20: Comparison of forecast and observation for all buses

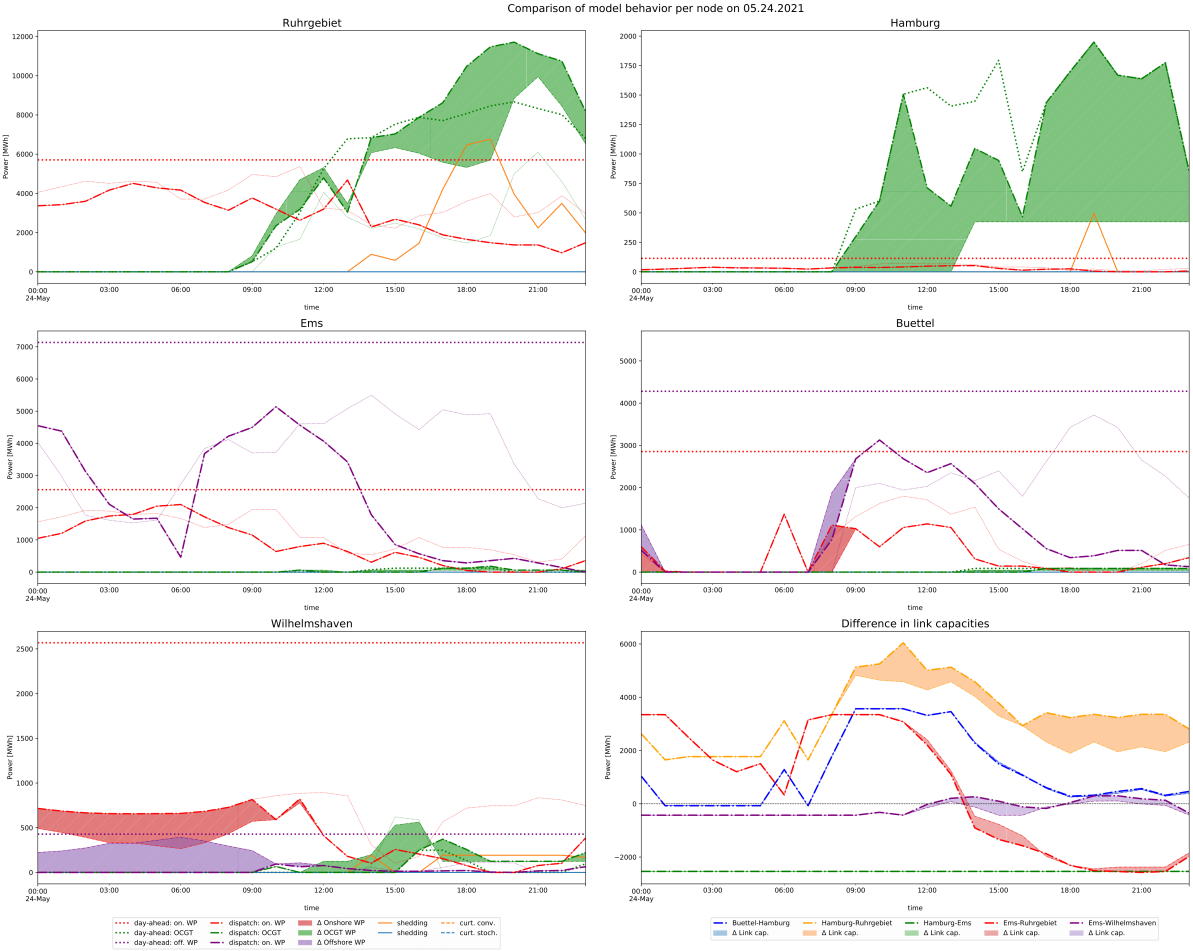

Figure 21: Comparison of model behavior for all buses

A.5 Impact of generator flexibility

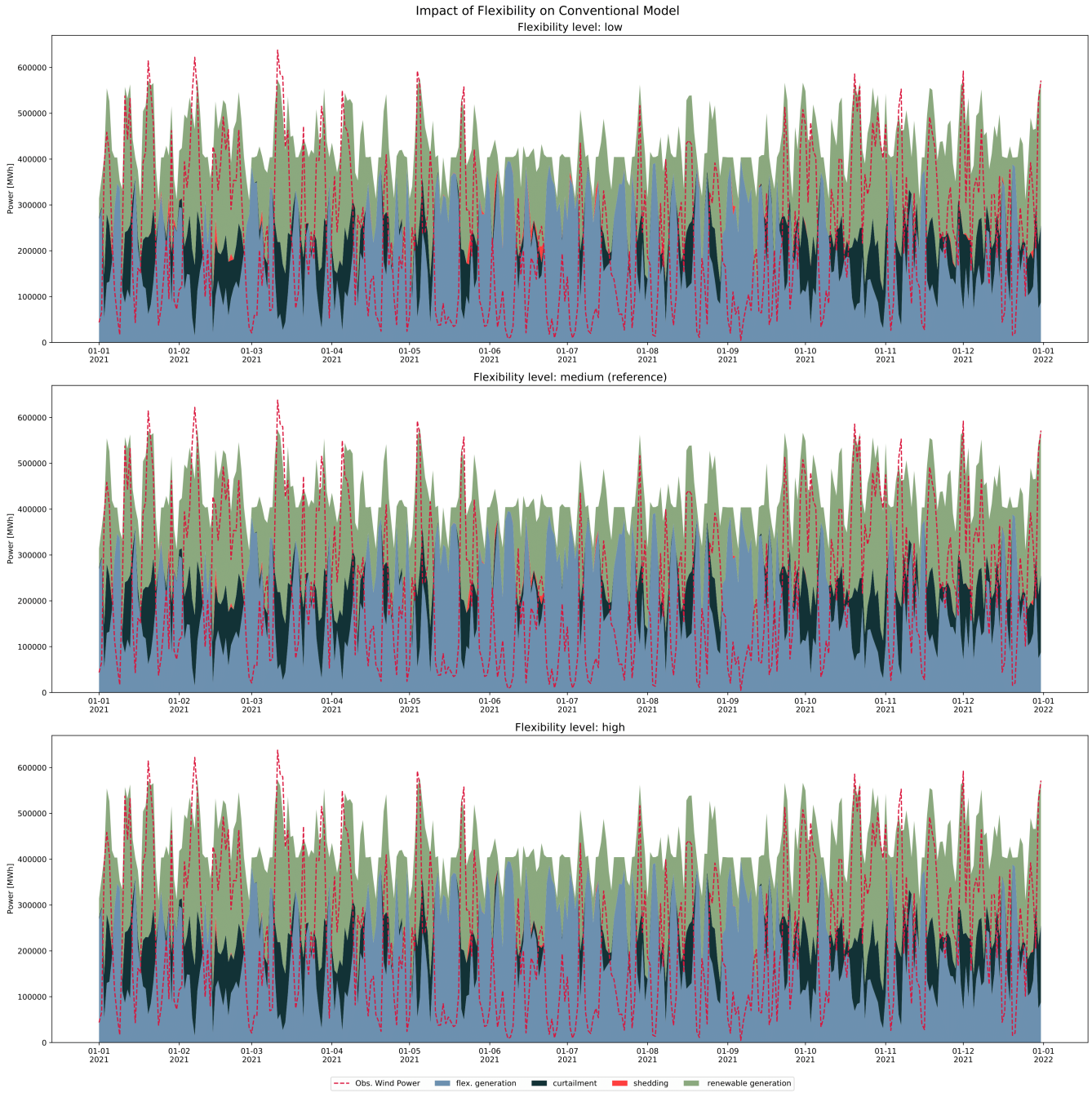

Figure 22: Comparison of impact of generator flexibility on conventional model.

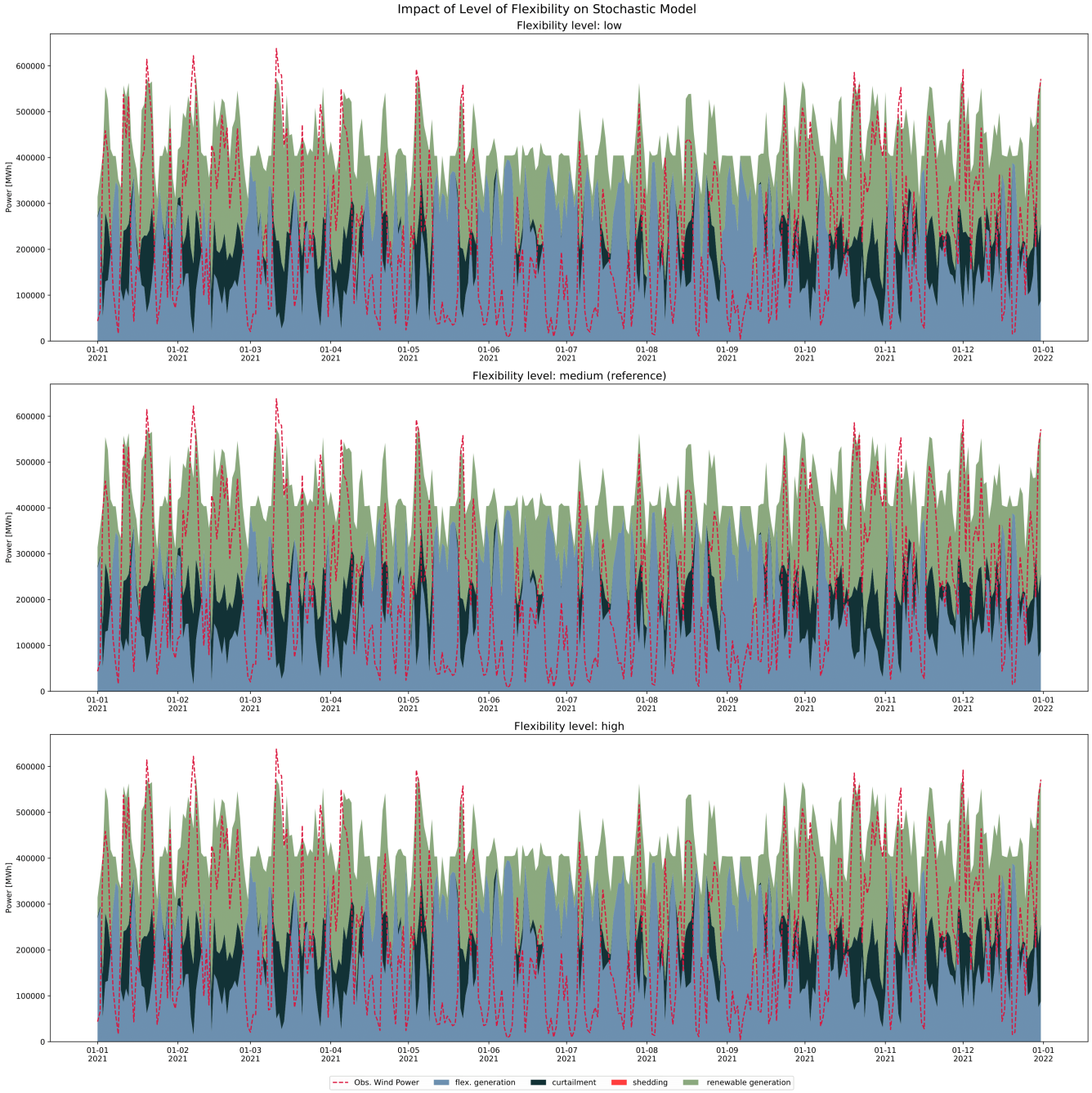

Figure 23: Comparison of impact of generator flexibility on stochastic model.

References

[1] D. I. A. McKay and et.al., "Exceeding 1.5°c global warming could trigger multiple climate tipping points", *Science*, 2022.

[2] L. Clarke and Y.-M. Wei, "Climate change 2022: Mitigation of climate change. contribution of working group iii to the sixth assessment report of the intergovernmental panel on climate change", Cambridge, UK and New York, USA, 2022.

[3] "World energy outlook 2022", *IEA*, pp. 137–138, 2022. [Online]. Available: https://www.iea.org/reports/world-energy-outlook-2022.

[4] C. Koch, *Levelized cost of electricity renewable energy rechnologies*, Freiburg, 2021.

[5] E. Bitar, R. Rajagopal, and et.al, "Bringing wind energy to market", vol. 27, no. 3, pp. 1225–1235, 2012. DOI: 10.1109/TPWRS.2012.2183395.

[6] A. van Stiphout, K. D. Vos, and G. Deconinck, "The impact of operating reserved on investment planning of renewable power systems", *IEEE Transactions on Power Systems*, vol. 32, no. 1, pp. 378–388, 2017. DOI: 10.1109/TPWRS.2016.2565058.

[7] P. Unruh, M. Nuschke, P. Strauß, and F. Welck, "Overview on grid-forming inverter control methods", *Energies*, vol. 13, no. 10, 2020. DOI: 10.3390/en13102589.

[8] E.Arriagada and et.al., "A stochastic economic dispatch model with renewable energies considering demand and generation uncertainties", pp. 1–6, 2013. DOI: 10.1109/PTC.2013.6652496.

[9] S. Weitemeyer, D. D. Kleinhans, L. Wienholt, D. T. Vogt, and P. D. C. Agert, "A european perspective: Potential of grid and storage for balancing renewable power systems", *Energy Technology*, vol. 4, pp. 114–122, 1 2016.

[10] J. Wen and et.al, "Transmission network expansion planning considering uncertainties in loads and renewable energy resources", *IEEE Electrical Power and Energy Conference*, 2016.

[11] J. Jurasz and et.al., "A review on the complementarity of renewable energy sources: Concept, metrics, application and future research directions", *Solar Energy*, vol. 195, pp. 703–724, 2020.

[12] T. Brown, D. Schlachtberger, A. Kies, S. Schramm, and M. Greiner, "Synergies of sector coupling and transmission reinforcement in a cost-optimised, highly renewable european energy system", *Energy*, vol. 160, pp. 720–739, 2018.

[13] J. Morales, M. Zugno, S. Pindea, and P. Pison, "Electricity market clearing with improved scheduling of stochastic production", *European Journal of Operational Research*, vol. 235, pp. 765–774, 3 2014.

[14] "Clearing the day-ahead market with a high penetration of stochastic production", in *Integrating Renewables in Electricity Markets - Operational Problems*. Springer, 2014, vol. 205, ch. 3, pp. 64–65, ISBN: 978-1-4614-9410-2.

[15] D. Wilks, "Stochastic forecasting", in *Statistical Methods in the Atmospheric Sciences*. Elsevier, 2006, ch. 6, pp. 229–236, ISBN: 9780127519661.

[16] C. Nicolis, "Probabilistic aspects of error growth in atmospheric dynamics", *Quarterly Journal of the Royal Meteorological Society*, vol. 118, pp. 415–595, 505 1992.

[17] ECMWF. "Ens-ensemble forecasts". (), [Online]. Available: https://confluence.ecmwf.int/display/FUG/ENS+-+Ensemble+Forecasts.

[18] H.-K. Ringkjob and et.al., "Towards improved understanding of the applicability of uncertainty forecasts in the electric power industry", *Energies*, pp. 1–8, 2017.

[19] L. Mones. "Using neural networks for predicting solutions to optimal power flow". (), [Online]. Available: https://invenia.github.io/blog/2021/10/11/opf-nn/.

[20] M. Cain, R. O'Neill, and A. Castillo, "History of optimal power flow and formulations", *49th IEEE Conference on Decision and Control (CDC)*, pp. 1051–1057, 2010.

[21] H. Liu and A. C. L. Tesfatsion, "Locational marginal pricing basics for restructured wholesale power markets", *Energy*, vol. 209, 2009.

[22] L. Mones, *A gentles introduction to optimal power flow*. [Online]. Available: https://invenia.github.io/blog/2021/06/18/opf-intro/#fn:Liu09.

[23] T. Brown, J. Hörsch, and D. Schlachtenberger, "Pypsa: Python for power system analysis", 2017.

[24] B. Schyska, "Coaction of input parameters and model sensitivities in numerical power system modeling", Ph.D. dissertation, 2021, ch. 2, pp. 3–5.

[25] *Pypsa documentation, power system optimization*. [Online]. Available: https://pypsa.readthedocs.io/en/latest/optimal_power_flow.html.

[26] E. Kraft, M. Russo, D. Keles, and V. Bertsch, "Stochastic optimization of trading strategies in sequential electricity markets", *European Journal of Operational Research*, vol. 308, pp. 400–421, 1 2023.

[27] J. Drücke and et. al., "Climatological analysis of solar and wind energy in germany using the grosswetterlagen classification", *Renewable Energy*, vol. 164, pp. 1254–1266, 2021.

[28] *Electricity demand for federal state*. [Online]. Available: https://openenergy-platform.org/api/v0/schema/demand/tables/ego_demand_federalstate/rows/.

[29] R. Sharma and J. Dhillon, "Pypsa: Open source python tool for load flow study", *Journal of Physics: Conference Series*, vol. 1854, 2021.

[30] M. Zamo and P. Naveau, "Estimation of the continuous ranked probability score with limited information and applications to ensemble weather forecasts", *Math Geosci*, vol. 50, pp. 209–234, 2018.

[31] "Loss of load expectation". (Apr. 2023), [Online]. Available: https://emissions-euets.com/internal-electricity-market-glossary/450-loss-of-load-expectation-lole.